

AD-A098 021

TEXAS UNIV AT EL PASO DEPT OF ELECTRICAL ENGINEERING F/G 17/8
EXTENDED APPLICABILITY OF OPTICAL WIND SENSING TECHNIQUES. (U)
FEB 81 J SMITH DAAG20-79-G-0072

UNCLASSIFIED

ERADCOM/ASL-CR-R1-0072-1 NL

1 OF 1
AD A
09802

END
DATE
FILMED
5-81
DTIC

ASL-CR-81-0072

ARO-16654.1-GS

AD

Reports Control Symbol
OSD 1366

AD A 098021

EXTENDED APPLICABILITY OF OPTICAL WIND SENSING TECHNIQUES

12

FEBRUARY 1981

LEVEL II

Prepared By
JACK SMITH

University of Texas at El Paso
Department of Electrical Engineering
El Paso, Texas 79968

UNDER CONTRACT NUMBER DAAG29-79-G-0072

Contract Monitor: ROBERTO RUBIO

Approved for public release; distribution unlimited



US Army Electronics Research and Development Command
ATMOSPHERIC SCIENCES LABORATORY
White Sands Missile Range, NM 88002

81 4 21 004

NOTICES

Disclaimers

The findings in this report are not to be construed as an official Department of the Army position, unless so designated by other authorized documents.

The citation of trade names and names of manufacturers in this report is not to be construed as official Government indorsement or approval of commercial products or services referenced herein.

Disposition

Destroy this report when it is no longer needed. Do not return it to the originator.

REPORT DOCUMENTATION PAGE		READ INSTRUCTIONS BEFORE COMPLETING FORM
1. REPORT NUMBER ASL CR-81-0072-1	2. GOVT ACCESSION NO. AD-A098 021	3. RECIPIENT'S CATALOG NUMBER
4. TITLE (and Subtitle) EXTENDED APPLICABILITY OF OPTICAL WIND SENSING TECHNIQUES		5. TYPE OF REPORT & PERIOD COVERED Final Report.
7. AUTHOR(s) Jack Smith		6. PERFORMING ORG. REPORT NUMBER
9. PERFORMING ORGANIZATION NAME AND ADDRESS The University of Texas at El Paso Department of Electrical Engineering El Paso, Texas 79968		8. CONTRACT OR GRANT NUMBER(s) DAAG29-79-G-0072
11. CONTROLLING OFFICE NAME AND ADDRESS US Army Electronics Research and Development Command Adelphi, MD 20783		10. PROGRAM ELEMENT, PROJECT, TASK AREA & WORK UNIT NUMBERS
14. MONITORING AGENCY NAME & ADDRESS (if different from Controlling Office) US Army Atmospheric Sciences Laboratory White Sands Missile Range, NM 88002		12. REPORT DATE February 1981
		13. NUMBER OF PAGES 53
		15. SECURITY CLASS. (of this report) UNCLASSIFIED
		15a. DECLASSIFICATION/DOWNGRADING SCHEDULE
16. DISTRIBUTION STATEMENT (of this Report) Approved for public release; distribution unlimited		
17. DISTRIBUTION STATEMENT (of the abstract entered in Block 20, if different from Report)		
18. SUPPLEMENTARY NOTES Contract Monitor: Roberto Rubio Grant number DAAG29-79-G-0072 covered the period from 1 July 1979 through 31 August 1980.		
19. KEY WORDS (Continue on reverse side if necessary and identify by block number) Scintillation Optical wind measurements Intensity Millimeter wave intensity fluctuations Fluctuations Temporal filtering of turbulence induced signals Atmospheric turbulence		
20. ABSTRACT (Continue on reverse side if necessary and identify by block number) The objectives of the study were to extend the applicability of optical crosswind sensing techniques to allow operation in rain and to determine the feasibility of using the techniques to study water vapor induced fluctuations at millimeter wavelengths.		

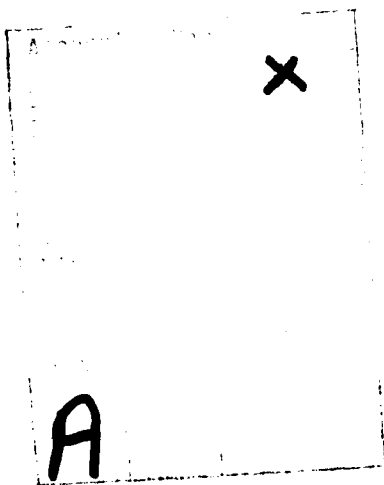
20. ABSTRACT (cont)

Two field tests were conducted to determine the effects of rain on optical crosswind sensors. The results showed that, (a) temporal filtering of the rain induced noise could improve the optical sensor performance under light rain conditions, (b) a simple frequency measurement of the fluctuating signal yielded a good representation of the windspeed variations, and (c) an improved turbulent signal to rain signal ratio can be obtained by using a receiver array to form a spatial filter. Temporal filtering imposes an upper limit on the speed which can be measured, but spatial filters would not have this limitation.

Wavelength scaling of intensity fluctuation observed at optical frequencies and at millimeter wave frequencies is used to obtain estimates of temperature and water vapor induced scintillations at millimeter and submillimeter wavelengths in the propagation windows. The estimated values are on the order of those observed in a 35 GHz propagation experiment.

CONTENTS

LIST OF FIGURES	4
1.0 Technical Summary	5
1.1 Statement of Problem	5
1.2 Field Tests Conducted	6
1.2.1 Holloman AFB Test	6
1.2.2 Beaverton, Oregon Test	9
1.2.3 Short Path Test	9
1.3 Test Results	12
1.3.1 Holloman AFB Test Results	12
1.3.2 Short Path Test Results	27
1.3.3 Beaverton Oregon Test Results	27
1.4 Discussion of Test Results	46
1.5 Scintillations at Millimeter Wavelengths	48
2.0 Important Results	52
3.0 References	53



LIST OF FIGURES

	Page
1. Holloman Test Site Schematic	8
2. Schematic of Beaverton, Oregon Field Test	10
3. Short Path Rain Test El Paso, Texas	11
4. Temporal Filtering Effects September 20 Test	13
5a-i. Optical Signal Spectra (Holloman)	14
6. Detected Optical Signals "Artificial Rain"	24
7. Temporal Filtering Effects October 10 Test	26
8. Filtering Effects - Heavy Rain	28
9. Short Path Test: Coherent Optical Signal January 31, 1980	29
10. Temporal Filtering Effects on Optically Determined Winds Noncoherent Source	30
11. Temporal Filtering Effects on Optically Determined Winds Coherent Source	31
12. Temporal Filtering Effects on Optically Determined Winds	33
13. Temporal Filtering Effects on Optically Determined Winds	34
14. Detected Optical Signals Natural Rain	36
15a-g. Optical Signal Spectra (Beaverton)	38
16. Expected Scintillation (Temperature Effects)	49
17. Expected Scintillation (Humidity Effects).	51

1.0 TECHNICAL SUMMARY

1.1 Statement of Problem

Observations of the fluctuating characteristics, i.e. intensity, phase, or position, of an optical beam have been used to determine "path averaged" turbulent intensity and the wind speed normal to the optical path^(1,2,3). The measurement techniques developed were based on the interaction of the optical beam with temperature induced random refractive index fluctuations. The effects of water vapor, mists and rain were neglected in calculating the interaction.

The major task of this study was to determine experimentally the effects of water in liquid and vapor form on the remote sensing of horizontal wind speeds and to test the effects of temporal filtering as a means of extending the use of the instruments over a greater range of weather conditions.

A secondary study was to determine the feasibility of using optical beam techniques at millimeter wavelengths. That is, would the signals obtained from millimeter wave fluctuations be suitable for the same type of instrumentation and processing as used by the optical systems? Extension of the optical techniques to the lower frequencies would allow examination of water vapor inhomogeneities and motion of these inhomogeneities. Estimates are made of the intensity fluctuations that might be expected due to small scale temperature and water vapor variations.

1.2 Field Tests Conducted

Two extensive field tests were conducted during the course of this work to determine the effects of rain on the optical wind measuring systems. Two different types of optical systems were tested. One system used a HeNe laser to provide a beam with a coherent wavefront. The second system employed a DC powered quartz-iodide lamp at the focal point of a Fresnel lens to provide a noncoherent wave.

The approach used to evaluate optical system performance was to make traditional in-situ measurements, anemometers, of the horizontal wind speed, temperature structure parameter, etc., at points along the path. Simultaneous analog recordings were made of these values along with the raw signals obtained from the optical detectors of the remote sensing systems. This technique provided a permanent, reusable data base.

Various data processing and filtering techniques were then applied to the recorded optical signals. The results, the wind speeds derived from the optical signals affected by various rain conditions, were then compared with the wind obtained from in-situ measurements.

Obtaining wind speed from the optical signals required the generation of an autocorrelation function, or the crosscorrelation function of the signals from a photodiode pair, or by measuring the frequency of the signal fluctuations.

1.2.1 Holloman AFB Test

During September and October, 1979 tests were run at the Rocket Sled Track at Holloman Air Force Base in Alamogordo, New Mexico.

The rocket track has a rain simulator field made up of separately controlled 400 foot sections.

The optical paths, 1 km in length, were positioned in the center of the track collinear with the line of sprinklers making up the rain field. A minimum of 400 feet and a maximum of 3,200 feet of the optical beam path could be subjected to "rain." The rain rate of the 400 foot sections was determined by the sprinkler size and as a consequence there was no control of rain rate within a sector. Fig. 1 illustrates schematically the test configuration and indicates the parameters recorded.

Several difficulties were encountered during the test including some which related to the use of test track rain field.

(a) The rain field is narrow and any cross winds tend to change markedly the amount of rain interacting with the beam.

(b) The noncoherent signal detector failed to operate properly, no data was obtained from this system.

(c) The rain field obtained its water from a storage tank. The size did not permit operating the rain field longer than about 20 minutes for the type of test run. After 20 minutes the test had to be halted and the tank refilled. Thus exposure to any given rain condition was shorter than desired.

(d) While the personnel at Holloman were very cooperative and provided all the assistance that could be expected, the nature of track scheduling was such that use of the track for periods longer than 3 - 4 hours was a problem.

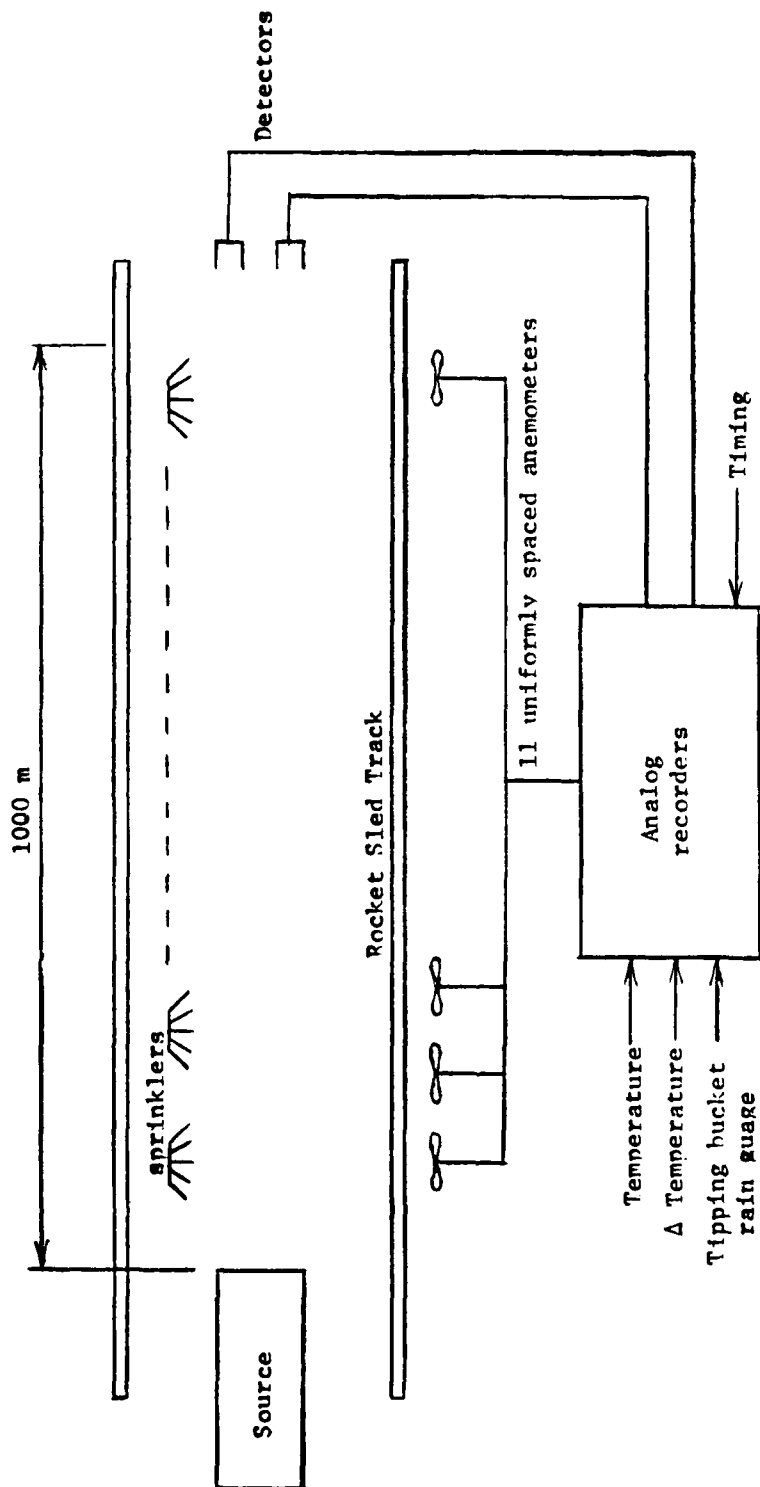


Fig. 1.
Holloman Test Site Schematic

1.2.2 Beaverton, Oregon Test

During late February and early March, 1980 a similar test was conducted near Beaverton, Oregon. The path length was 1 km and the beam path height was about 2 meters above a plowed farm field. As in the previous tests a permanent data record was obtained by simultaneously recording signals from five anemometers spaced along the path, from detectors viewing a coherent light source, from detectors viewing an incoherent light source, and from recording of temperature, temperature differentials, relative humidity, and rain rate. Figure 2 illustrates the field test configuration. The Oregon test site in February-March was chosen as there was a higher probability of rain and fog than at most other suitable domestic locations. The Oregon Graduate Center allowed use of their experimental site and some facilities.

The purpose of this experiment was to evaluate performance of optical wind sensors under natural rain conditions. Unfortunately the time available for the field test proved to be too short. The weather was generally overcast but only a few light rain situations accompanied by light winds were encountered.

1.2.3 Short Path-Test

A third simple test was conducted over a 40 meter path during a heavy rain in El Paso, Texas in late January, 1980. Figure 3 illustrates the path geometry. In this experiment no anemometer speeds were available for comparison with the speeds obtained optically. The recorded signals were processed to test the effects of temporal filtering on the shape of the wind profile obtained from the fluctuating beam characteristics when the beam interacted with rain.

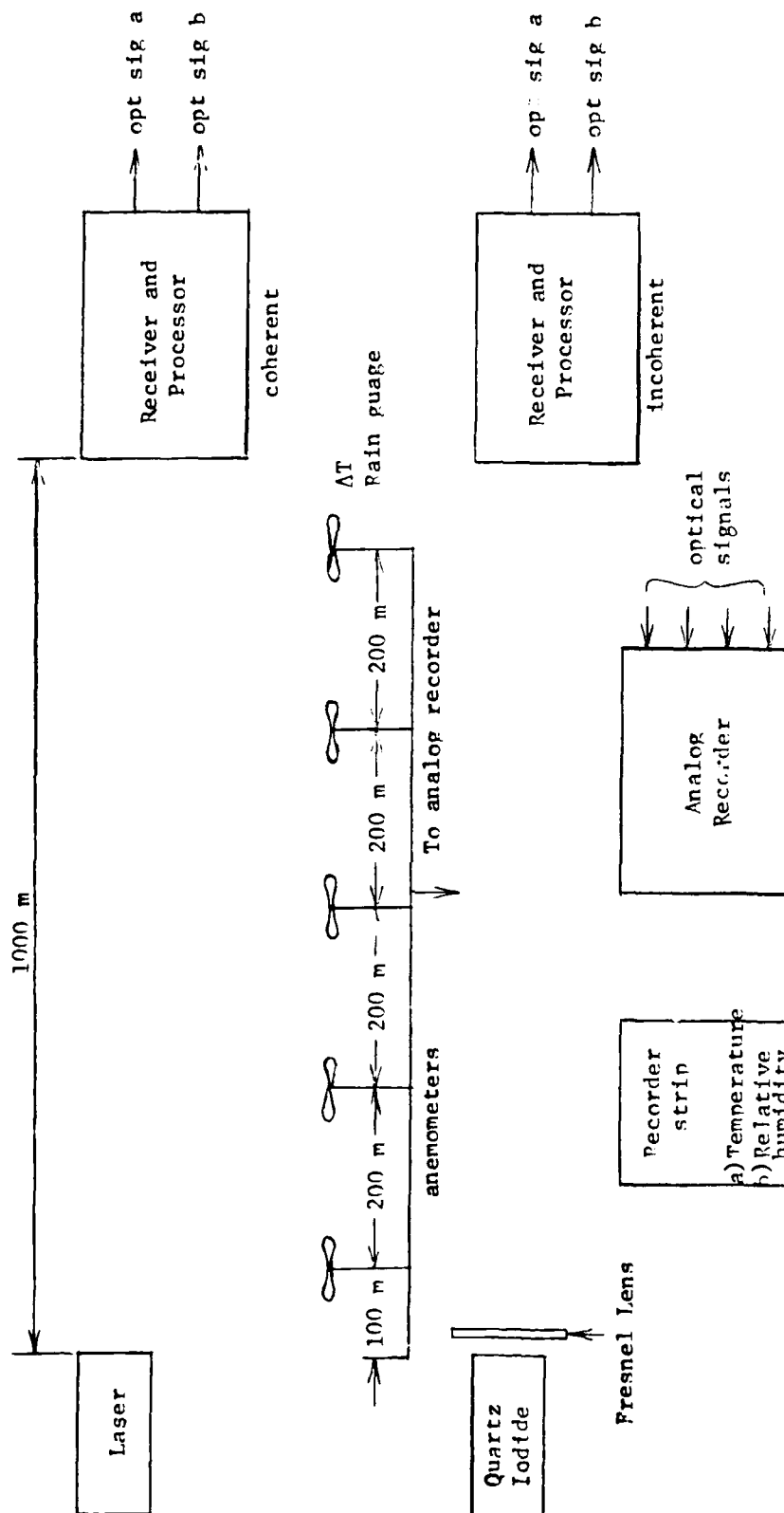


Fig. 2.
Schematic of Beaverton, Oregon Field Test.

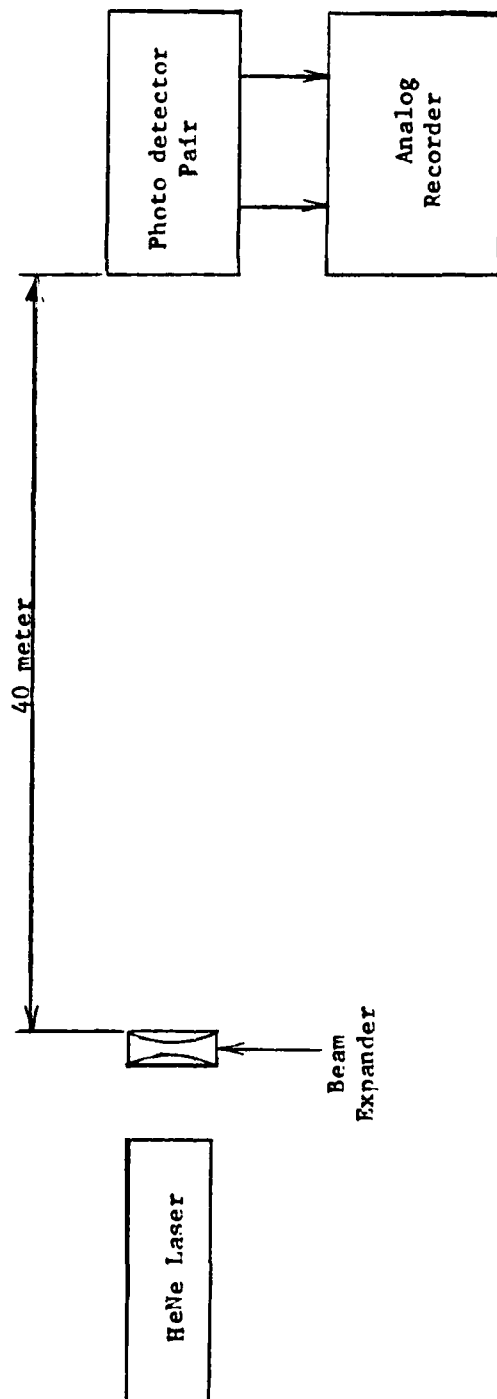


Fig. 3. Short Path Rain Test
El Paso, Texas

1.3 Test Results

1.3.1 Holloman AFB Results

Figure 4 was obtained from the results of the field test conducted under the "artificial rain" conditions at Holloman Air Force Base on September 20, 1980. This represents a result typical of the field test results obtained at Holloman. The sprinkler heads used had a calculated rain rate of 2.5 in/hr.

The figure compares the shapes of the wind profiles obtained from the optical signals with the wind speeds measured by an anemometer. The optical signals were fed through low pass filters with preselected upper cutoff frequencies, and then the wind speed fluctuations were obtained by electronically measuring the changes in the zero crossing frequency or the changes in the value of a correlation function. The length of the "rain path" and a qualitative description of the beam intensity is noted along the horizontal axis of the figure. The data indicate:

(a) In the presence of rain, as determined by the weak signal condition, the speeds obtained from the unfiltered optical signals tend to peak markedly.

(b) Using a 150 Hz low pass filter, and using the zero crossing frequency as a measure of speed, yielded results which most closely resembled the anemometer speed fluctuations.

The optical signal data from September 20, were also analyzed to determine the frequency content. Samples of these spectra are shown in Figs. 5 (a) through 5(i). As expected, the presence of rain

September 20, 1979
Holloman, AM
Coherent Optical Beam Source

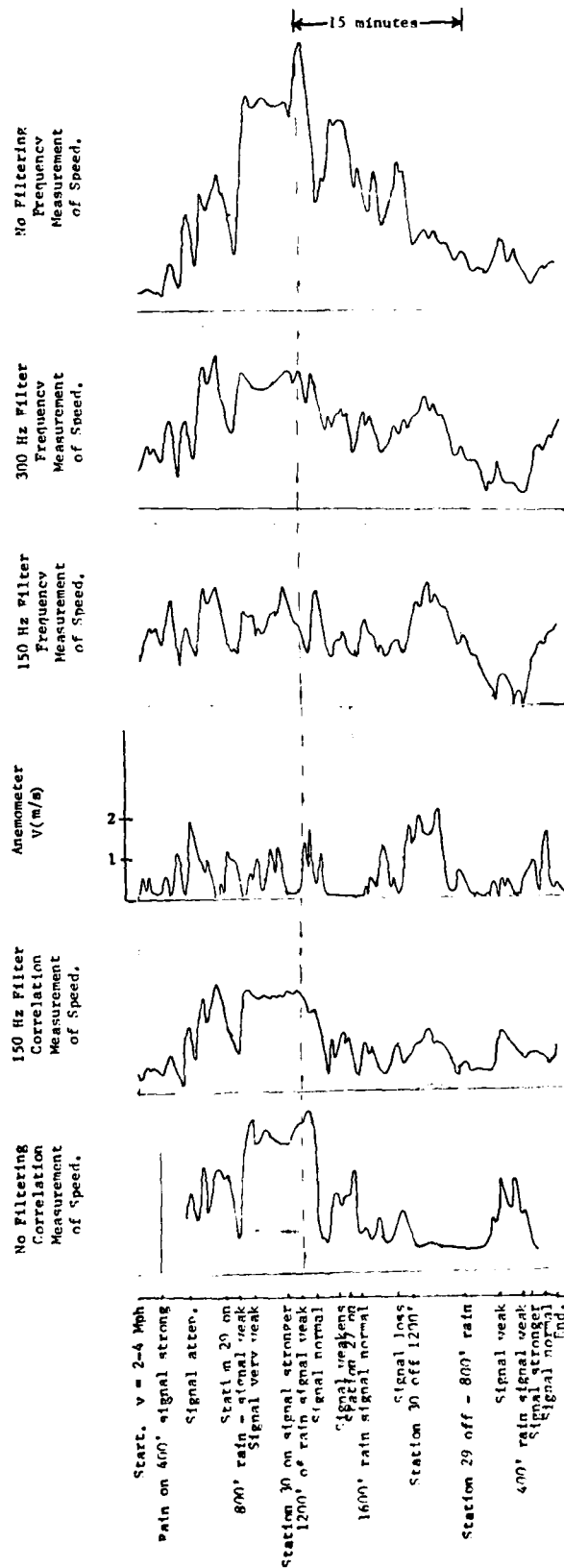


Figure 4. Temporal Filtering Effects September 20 Test.

OX5B
 TAPE: CH #4
 Signal Strong - Rain field off
 Coherent Optical Signal
 Data Date: Sept. 20, 1979
 Time - 21:11:00 → 21:11:45

Bandwidth: 30 Hz
 Freq. Span/div: 0.2 KHz
 Sweep Time: 5 sec
 Input Sens: 10 V
 Amp mode: 10 db

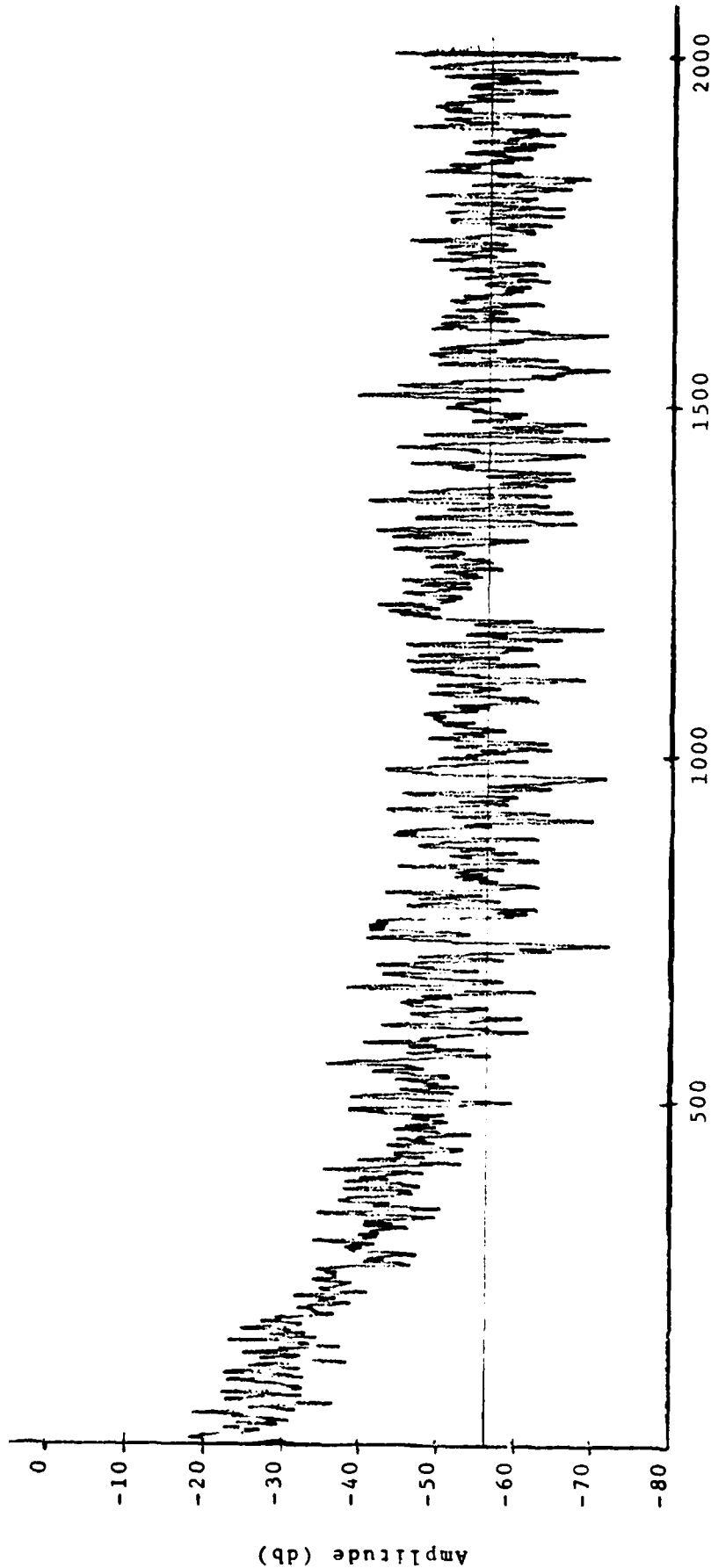
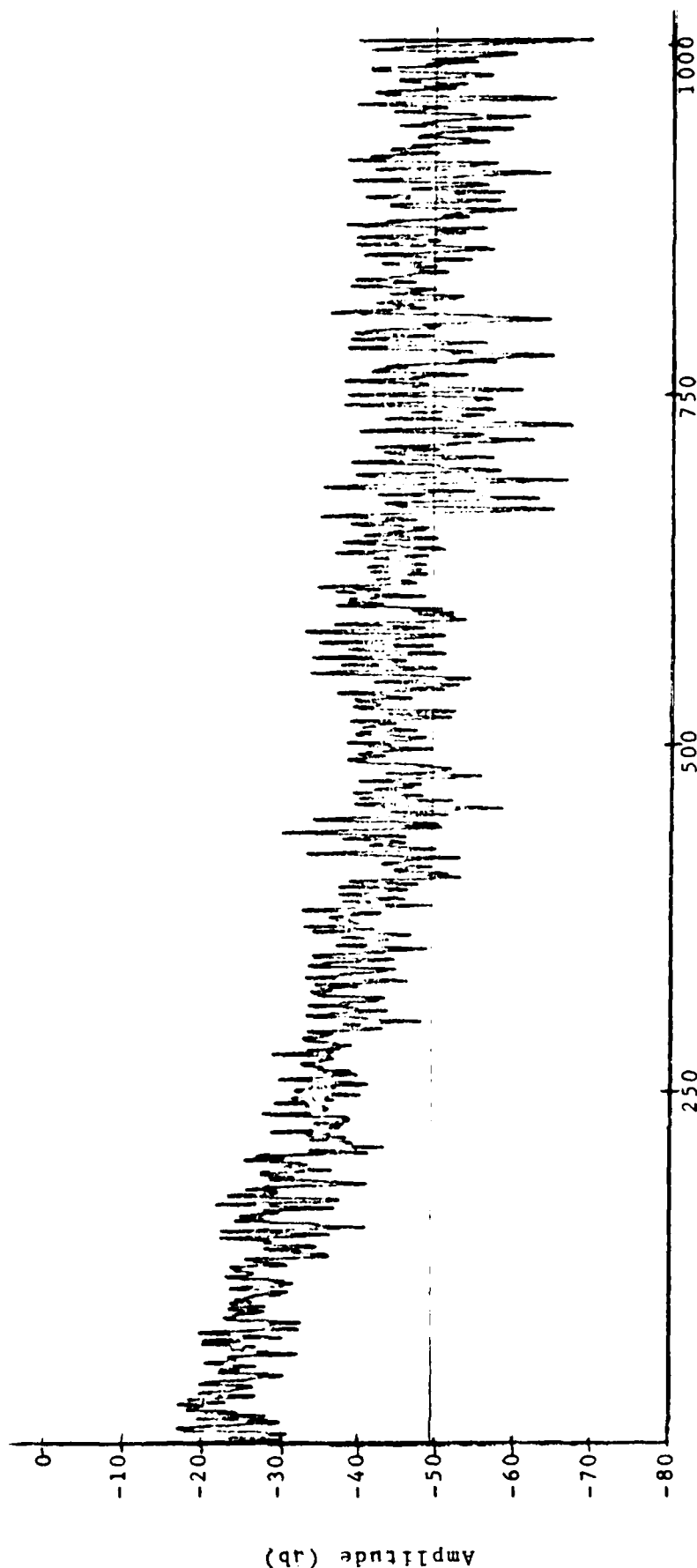


Fig. 5a.
 Optical Signal Spectra (Holloman)

OX53
 TAPE: CH #4
 Signal Strong - rain fld. off
 Coherent Optical Signal
 Data Date: Sept. 20, 1979
 Time - 21:11:00 → 21:11:45
 Exp. 7.5 in/s

Bandwidth: 30 Hz
 Freq. Span/div: .1 KHz
 Sweep Time: 5 sec
 Input Sens: 10 V
 Amp mode: 10 db



Frequency (Hz)

Fig. 5h.

OX5B
 TAPE: CH #4
 Signal Near Normal ~ 400 ft. of rain
 Data Date: Sept. 20, 1979
 Time - 21:49:45 → 21:50:30
 Exp. 7.5 in/s

Bandwidth: 30 Hz
 Freq. Span/div: .1 KHz
 Sweep Time: 5 sec
 Input Sens: 10 V
 Amp mode: 10 db

Wind Speed ~ 1 m/s



Frequency (Hz)

Fig. 5c.

OX5B
 TAPE: CH #4
 Signal Level Damped - 400 ft. of rain
 Coherent Optical Signal
 Date: Sept. 20, 1979
 Time - 21:16:00 + 21:16:45
 Exp. 7.5 in/s

Bandwidth: 30 Hz
 Freq. Span/div: .1 KHz
 Sweep Time: 5 sec
 Input Sens: 10 V
 Amp mode: 10 db

Wind Speed ~ 0 m/s

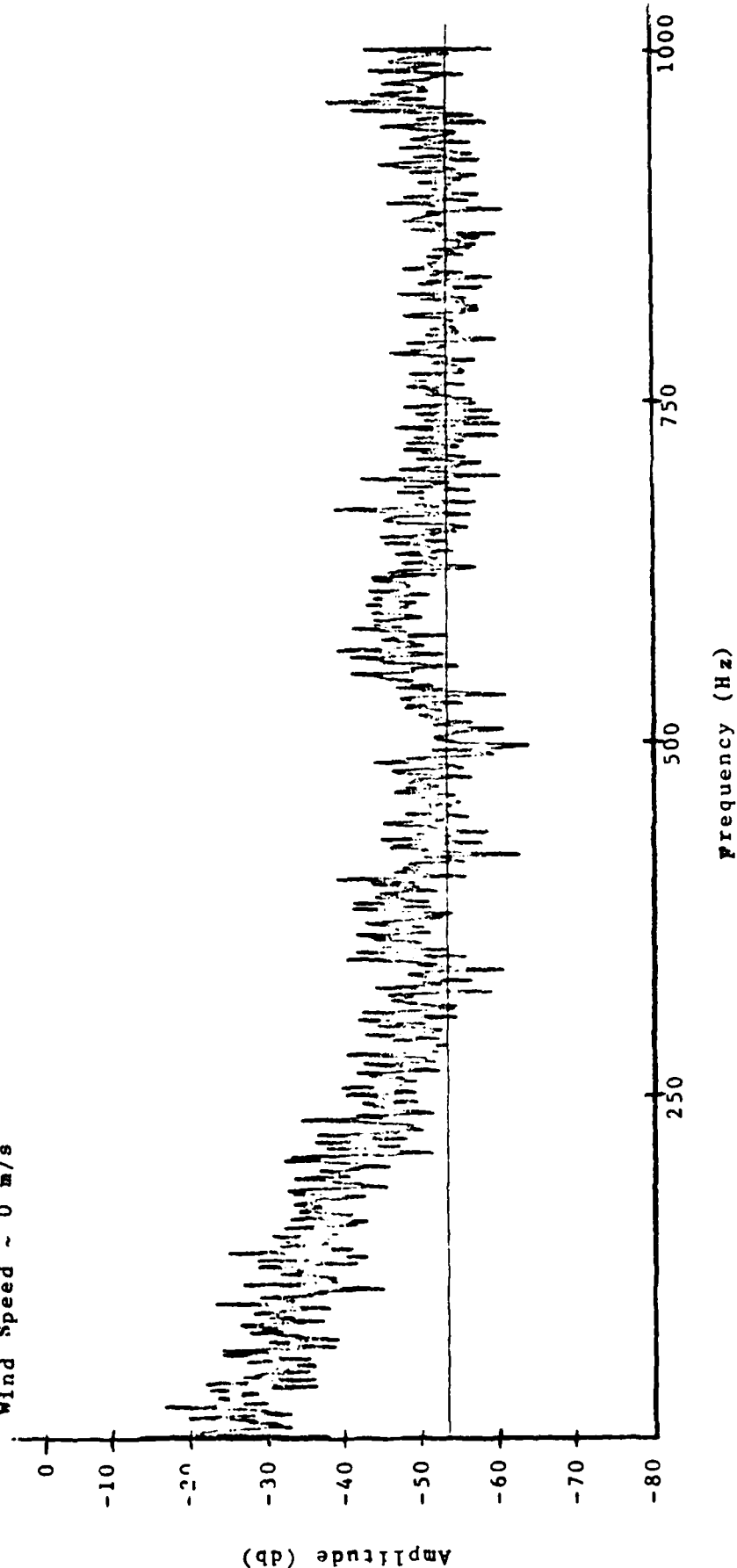


Fig. 5d.

OX5B
 TAPE: CH #4
 Signal Damped - 800 ft. of rain
 Coherent Optical Signal
 Data Date: Sept. 20, 1979
 Time - 21:21:35 + 21:22:05
 Exp. 7.5 in/s

Wind Speed 0-1 m/s variable

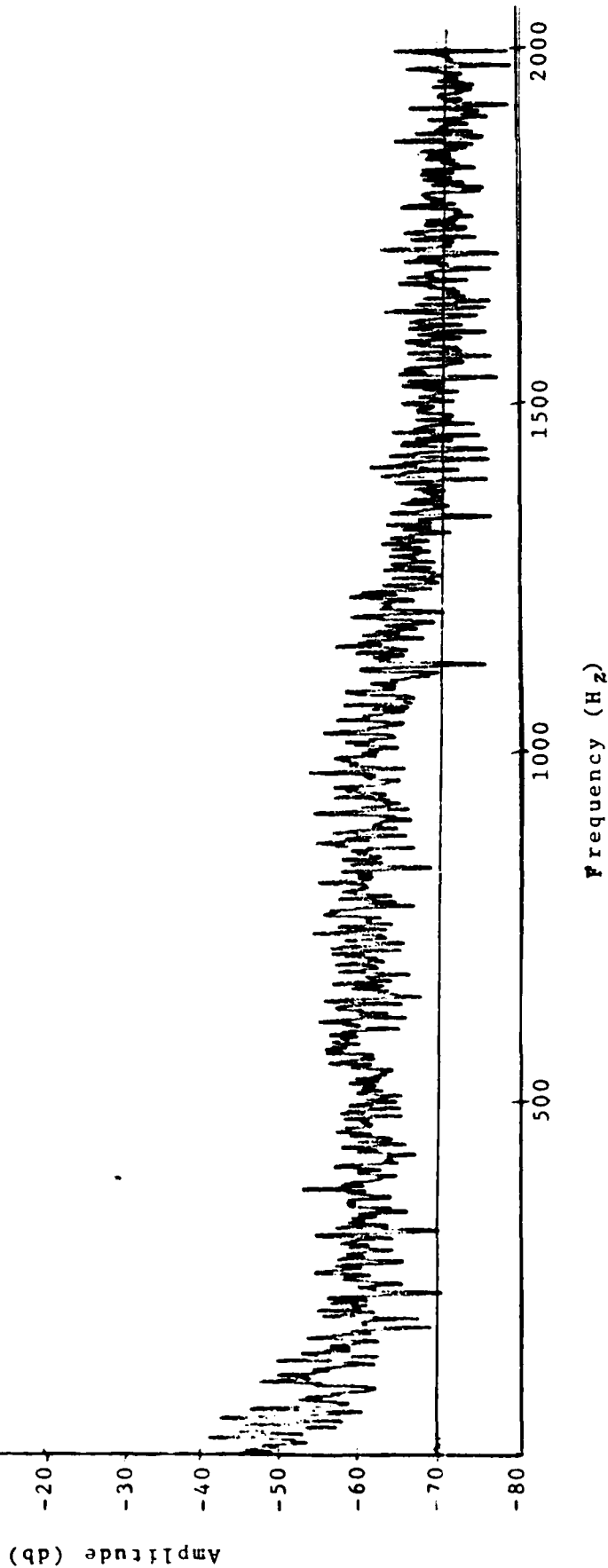
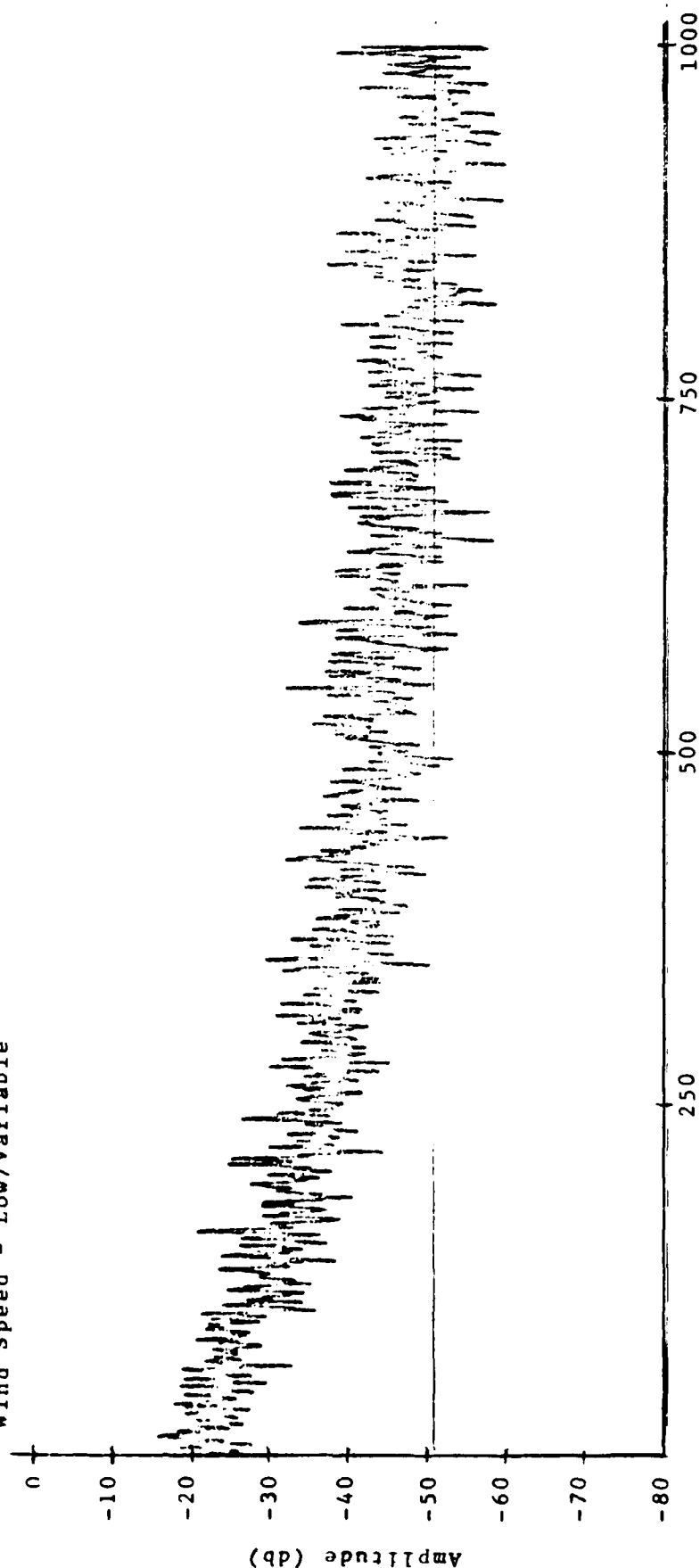


Fig. 5e.

OX5B
 TAPE: CH #4
 Signal Strong but Intermittently
 Damped - 800 ft. of rain
 Coherent Optical Signal
 Data Date: Sept. 20, 1979
 Time - 21:41:45 + 21:42:30
 Exp. 7.5 in/s
 Wind Speed - Low/Variable

Bandwidth: 30 Hz
 Freq. Span/div: .1 KHz
 Sweep Time: 5 sec
 Input Sens: 10 V
 Amp Mode: 10 db



Frequency (Hz)

Fig. 5f.

OX5B

Tape: CH #4

Signal Nearly Extinguished - 800 ft. of rain

Coherent Optical Signal

Date Date: Sept. 20, 1979

Time - 21:46:05 - 21:46:50

Exp. 7.5 in/s

Bandwidth: 30 Hz
Freq. Span/div: .1 KHz
Sweep Time: 5 sec
Input Sens: 10 V
Amp Mode: 10 db

Wind Speed \approx 0 m/s

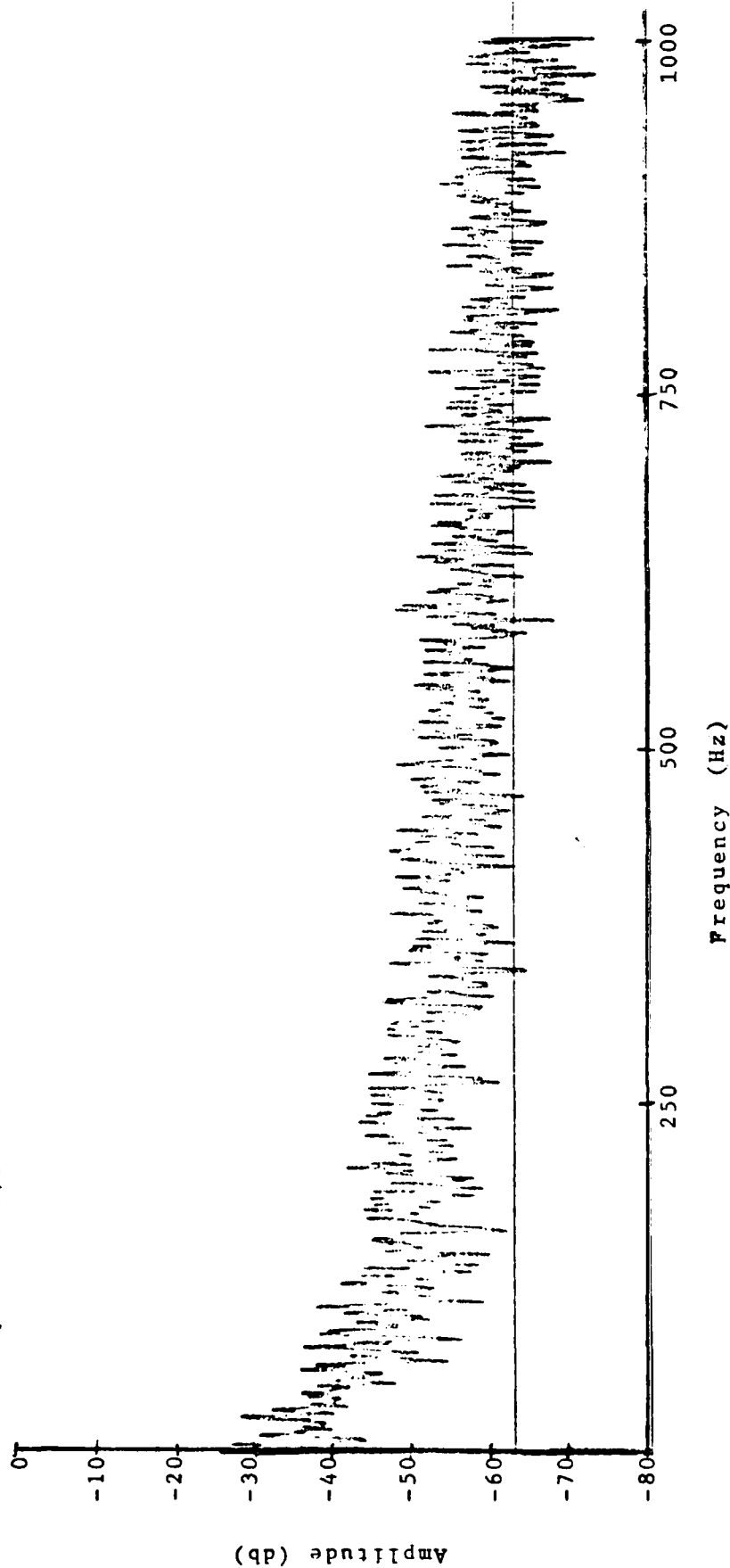
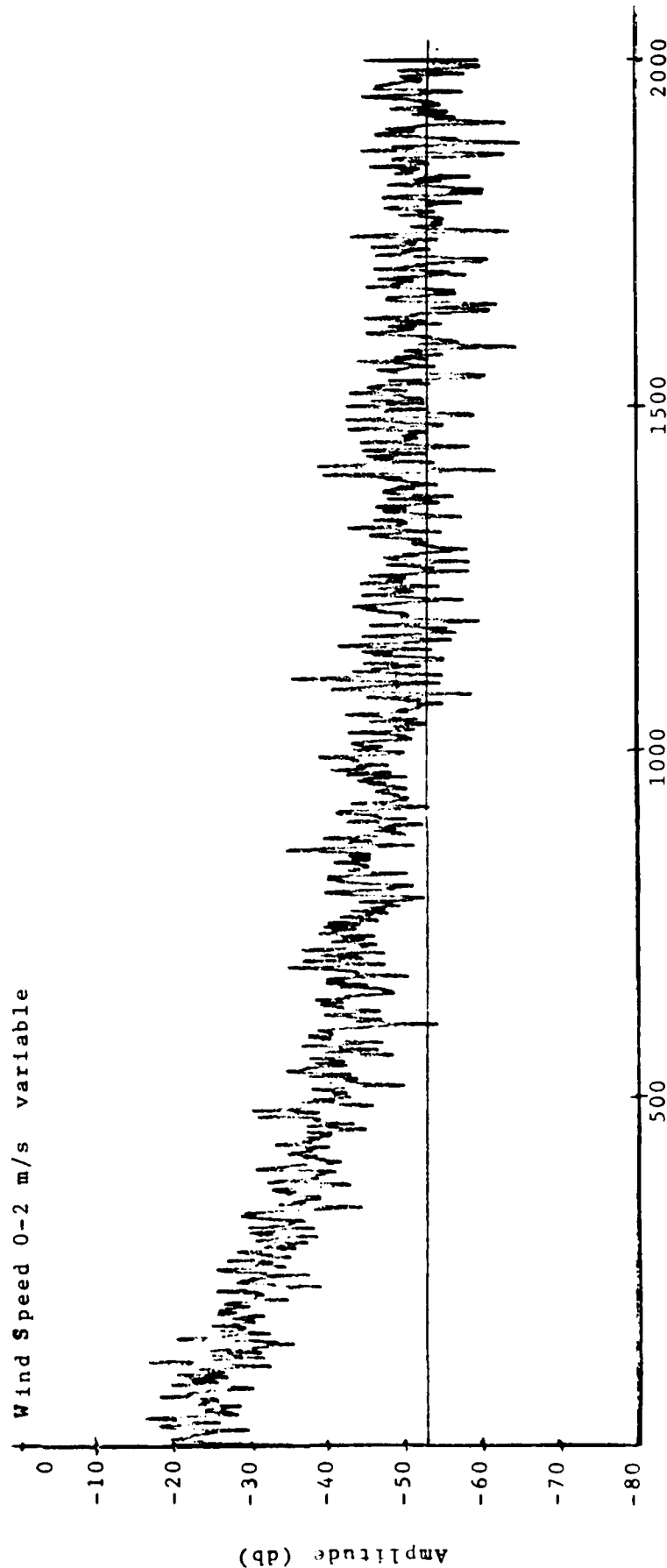


Fig. 58.

OX5B
 TAPE: CH #4
 Signal Strength and Shape near Normal -
 1200 ft. of rain
 Coherent Optical Signal
 Data Date: Sept. 20, 1979
 Time - 21:37:00 + 21:37:45
 Exp. 7.5 in/s

Bandwidth: 30 Hz
 Freq. Span/div: 0.2 KHz
 Sweep Time: 5 sec
 Input Sens: 10 V
 Amp mode: 10 db

Wind Speed 0-2 m/s variable



Frequency (Hz)

Fig. 5h.

Bandwidth: 30 Hz
 Freq. Span/div: 0.2 KHz
 Sweep Time: 5 sec
 Input Sens: 10 V
 Amp Mode: 10 db

OX5B
 TAPE: CH #4
 Signal Level Low - 1200 ft. of rain
 Coherent Optical Signal
 Data Date: Sept. 20, 1979
 Time - 21:24:45 → 21:25:30
 Exp. 7.5 in/s

Wind Speed ~ 0 m/s

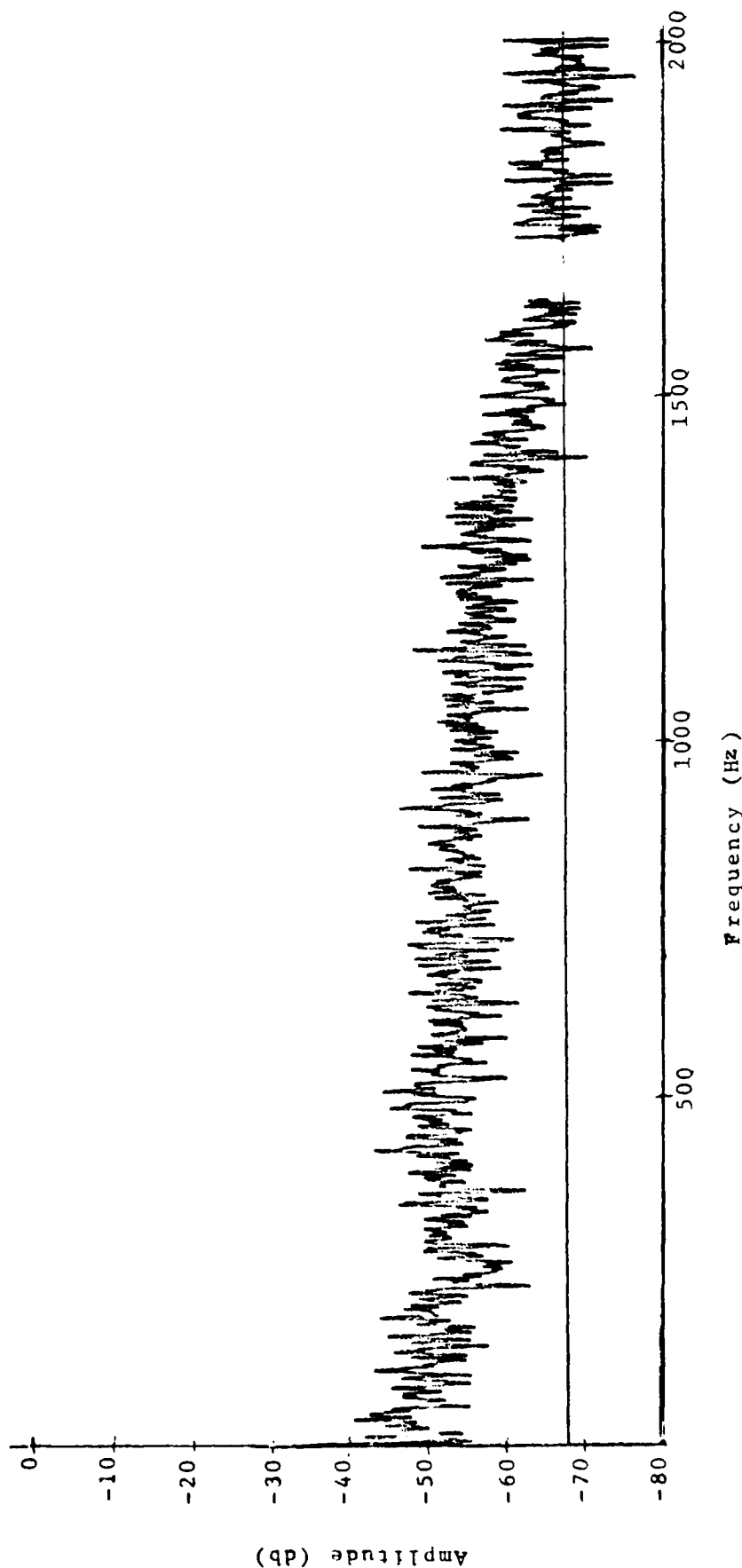


Fig. 51.

added high frequency components to the lower frequency components induced by the turbulence.

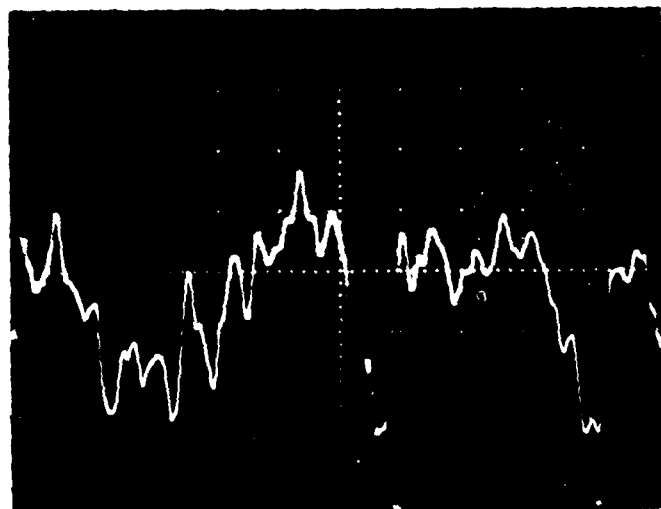
From the data it appears that as the beam interacts with more water the detected signals develop flatter spectra, i.e., comparatively less than normal portion of energy at low frequencies relative to the high frequencies. The presence of the rain induced frequencies will void the calibration of the remote wind sensing processor.

Figures 6(a) through 6(c) are photographs of optical signals detected when the coherent signal beam interacts with increasing amounts of rain. The drop size and velocity produced small amplitude spikes about 4 m wide at the base.

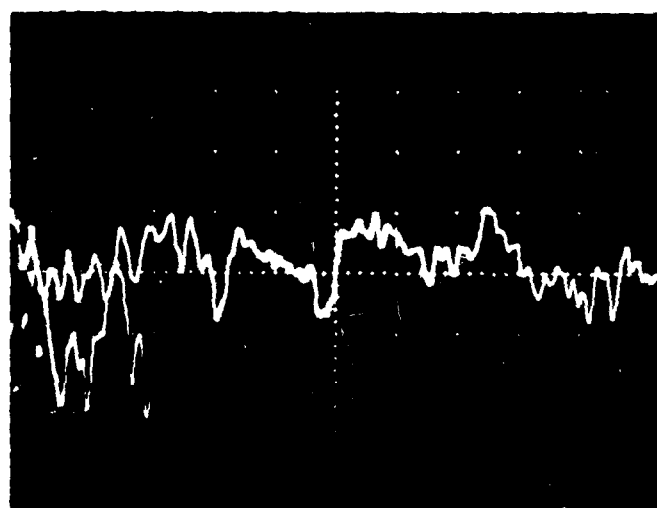
There was a basic problem in the use of the narrow rain field at the sled track. Any crosswind velocity tended to carry the rain out of the optical beam. Therefore, only weak interaction was obtained when wind speeds were high. Significant rain-beam interaction occurred when the winds were calm. The effects of variable winds on the position of the rain relative to the optical beam prevented any detailed analysis of the signal spectra vs. the rain path length.

A second example of results obtained from tests conducted at Holloman AFB is shown in Fig. 7. The data were obtained on October 10. The sprinkler heads were different from the September 20 tests, and the heads had a calculated 2.2 in/h rain rate. Additionally the maximum rain path was increased to 3200'.

The speed results obtained from the optical signals are about the same as those illustrated by results previously discussed. The zero crossing frequency measurement of the "300 Hz" filtered optical

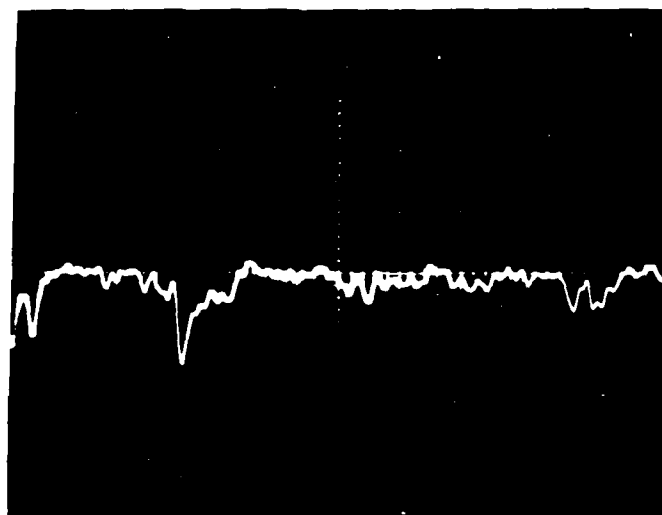


(a)



(b)

Fig. 6
Generated optical "noise"
"Artificial "and"



(c)

Sweep Speed 20 ms/cm
Sensitivity 0.5 V/cm
for photographs (a), (b), (c)

Fig. 6.

Detected Optical Signals
"Artificial Rain"

October 10, 1979
Holloman, AFB
Coherent Optical Beam Source

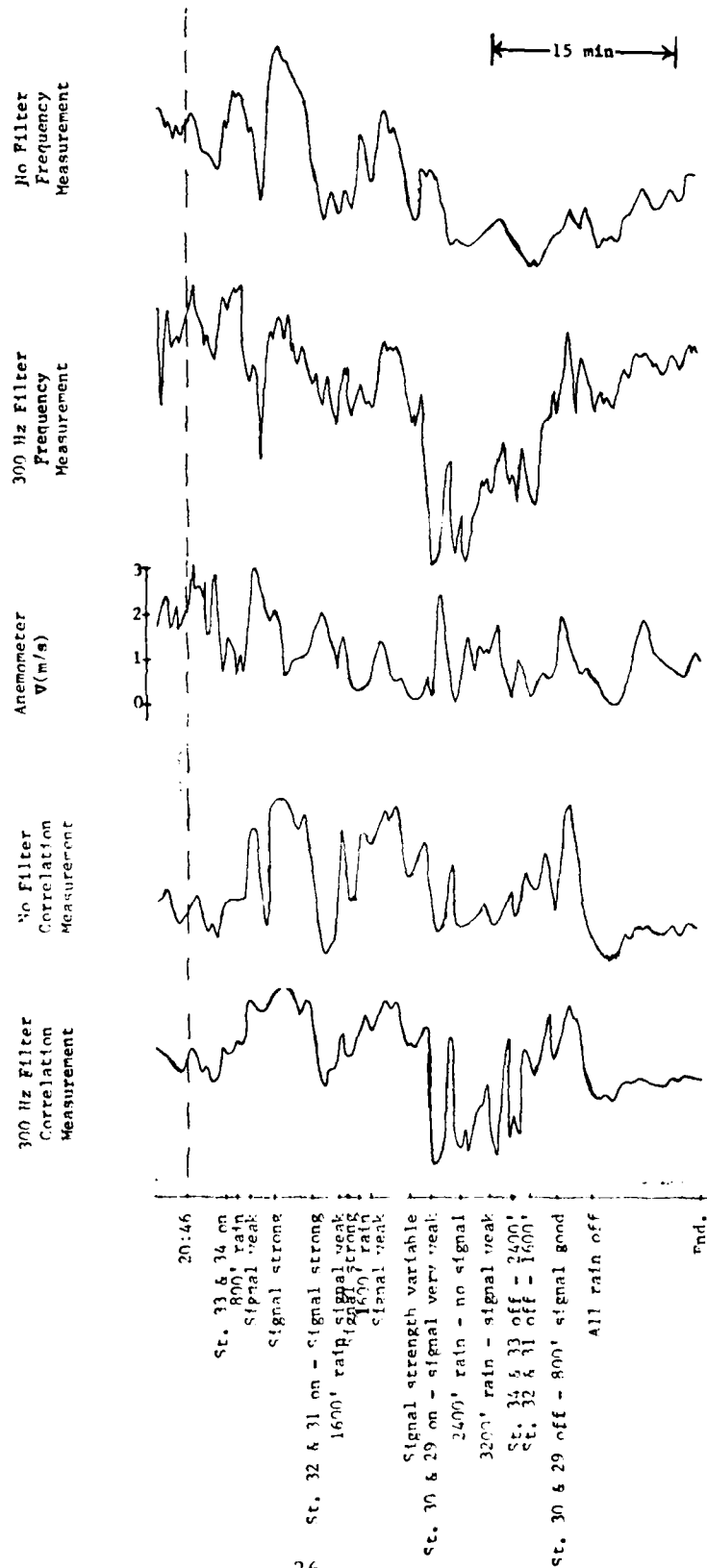


Fig. 7.
Temporal Filtering Effects
October 10 Test

signal yielded a speed curve most like the speed fluctuations of the anemometer. Again, optical measurements under conditions of weak signal (in this case there is strong interaction between the rain and the beam) produced poor results in all processing and filtering schemes. Unfortunately the experimental conditions did not allow obtaining data which could be used to determine the minimum "signal/noise" required for satisfactory optical instrument operation.

1.3.2 Short Path Results

Results of the short path experiment in which the coherent optical beam interacted with a relatively heavy rain are shown in Fig. 8. The effects of low pass filtering on the correlation measurement to obtain wind speed are demonstrated. Figure 9 contains photographs showing the signal under rain, (a), and no rain, (b), conditions. The spectra obtained from the signals detected during this test exhibited about 10db stronger components between 600 and 1200 Hz when the beam was affected by the rain.

1.3.3 Beaverton Oregon Results

The tests in late February and early March did not provide the variety of weather conditions which were initially anticipated. In general there were periods of light rain, some mist, but no fog was encountered during the experimental runs.

The results obtained on March 3 and 4, shown in Figs. 10 and 11, compare the anemometer measured wind speeds with those obtained from beams generated by noncoherent and coherent optical sources. Figure 10, shows the wind speed profile obtained by counting the

January 31, 1980
Short path "40" m - Coherent Beam
Correlation Measurement of Speed

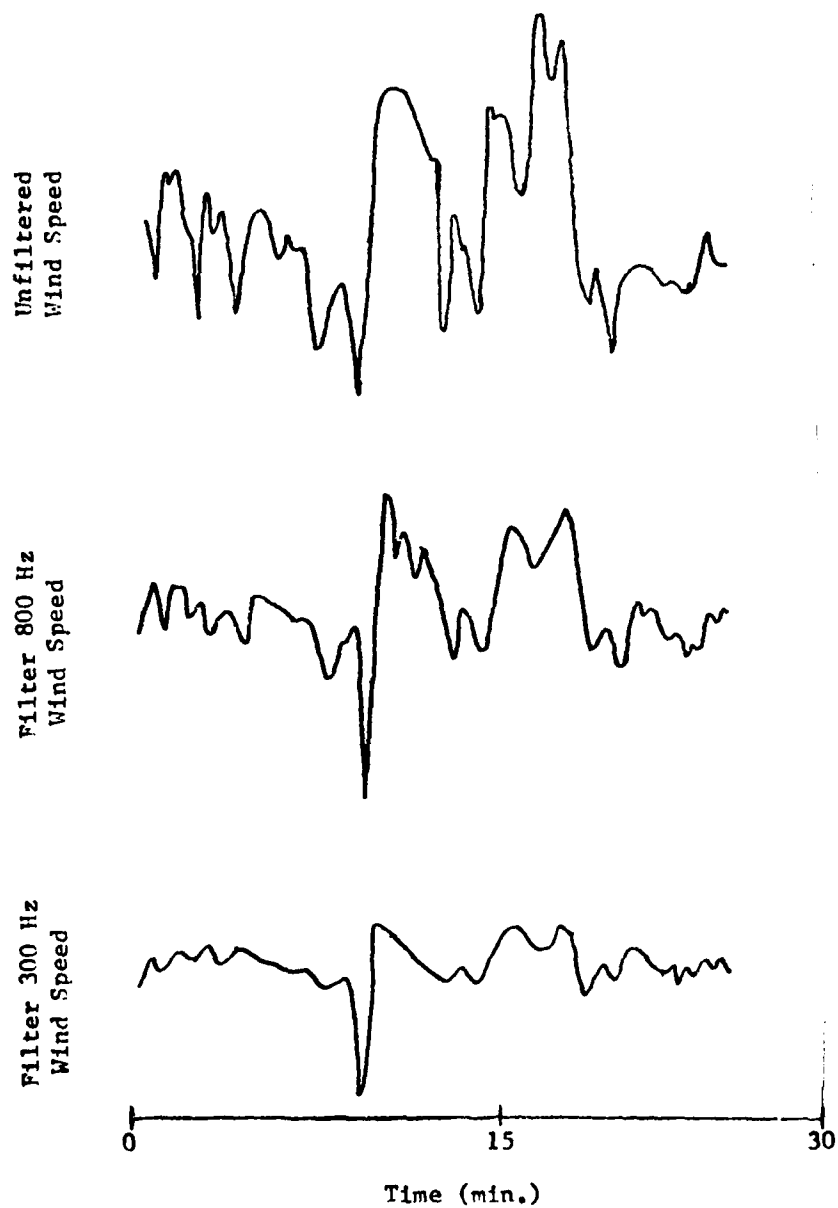
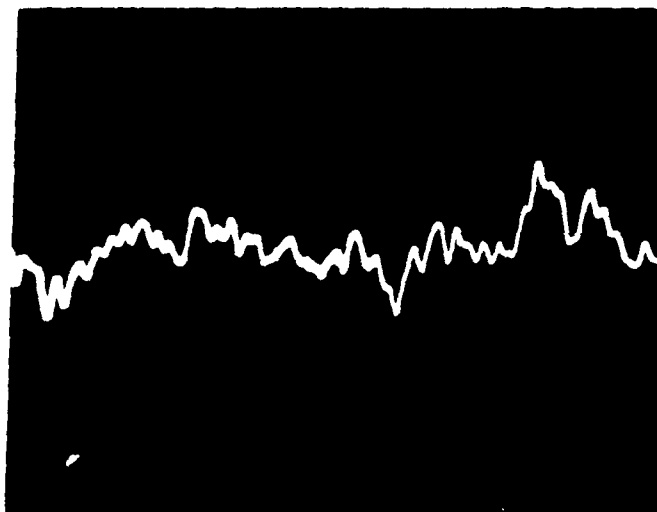
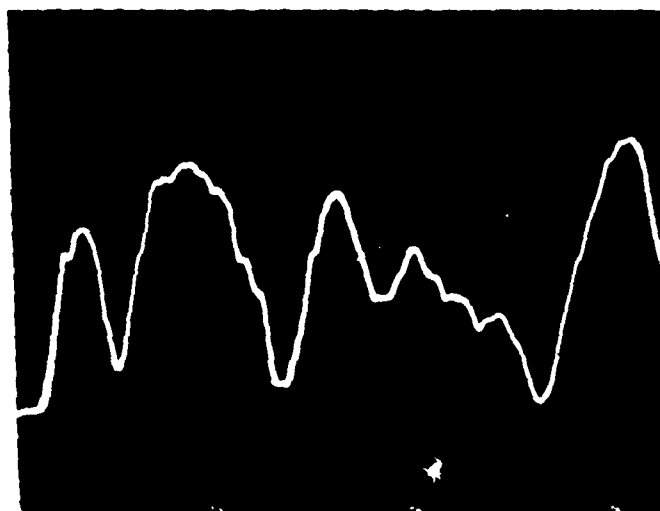


Fig. 8.

Filtering Effects: - Heavy Rain



Rain (a)
20 ms/cm Sweep: 0.5 V/cm Sensitivity
for (a) and (b)



No Rain (b)

Fig. 9

Short Path Test: Coherent Optical Signal
January 31, 1980

March 3-4, 1980
Beaverton, Oregon

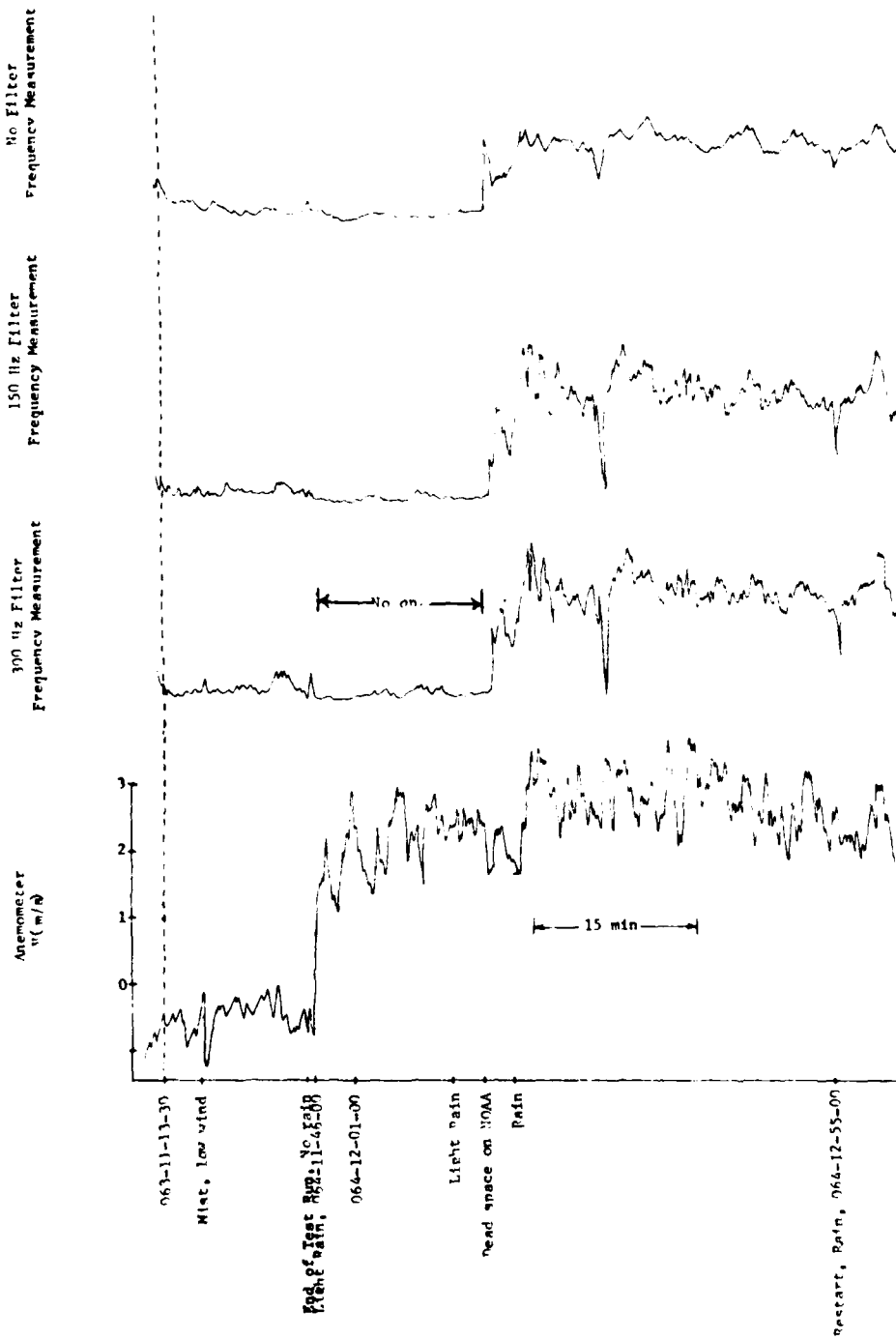


Figure 10. Temporal Filtering Effects on Optically Determined Winds Noncoherent Source.

March 3-4, 1980
 Beaverton, Oregon

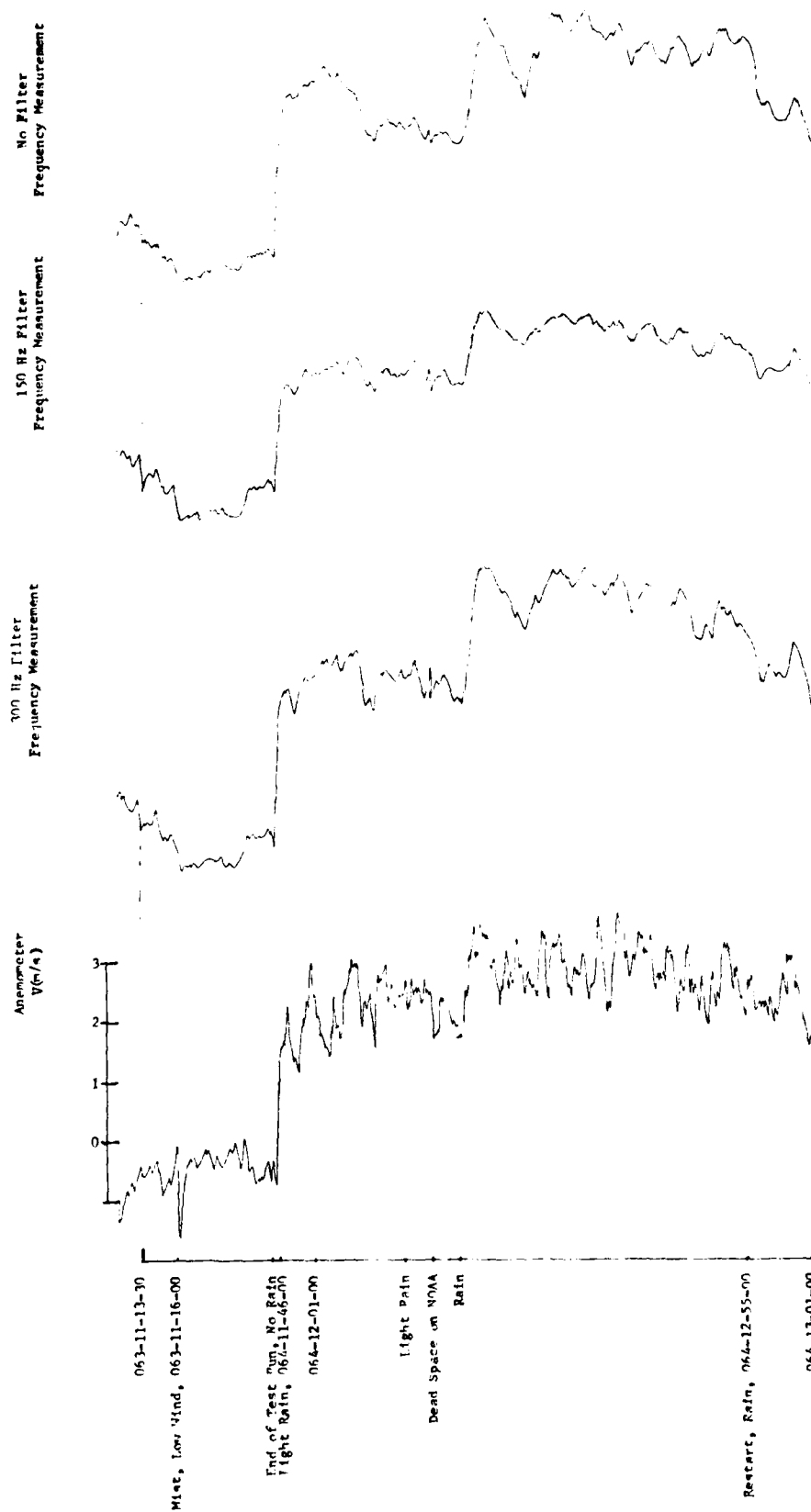


Figure 11. Temporal Filtering Effects on Optically Determined Winds Coherent Source.

zero crossings of the noncoherent signal. During the 2nd quarter of the run the electronics ~~was~~ not operating properly. When the system was operational there appears to be little difference in the curve shapes, but low pass filtering of the optical signals to 300 Hz produces a somewhat better speed profile, like that of the anemometer speeds, and is preferred over 150 Hz filtering. This conclusion also holds for the results obtained from the coherent optical signals, Fig. 11.

During the above tests the rains were light, trace to about .01 in/hr. The temperature was about 50° F. While there was fog in the general area, none was observed at the test site. The rain was too light to have much if any effect on the wind results from the optical processors.

Figure 12 compares the wind profiles resulting from a zero crossing count of intensity fluctuations obtained from the detector viewing a noncoherent optical beam with the results obtained from a midpath anemometer. While the light rain did not greatly affect the optical system results, the filtering above 300 Hz produced the best match to the anemometer result. The optical signal processing produces only the magnitude of the speed, whereas the anemometer also gave direction. Figure 13 continues the March 10th, data which later in the day exhibited light rain but higher winds than previously recorded. Wind profiles were determined from a zero crossing count and from a correlation measurement of the fluctuations of the coherent optical signals. In this case the unfiltered signal and 300 Hz filtered version applied to the correlation measurement gave the best

March 7-10, 1980
 Beaverton, Oregon
 Tape #2

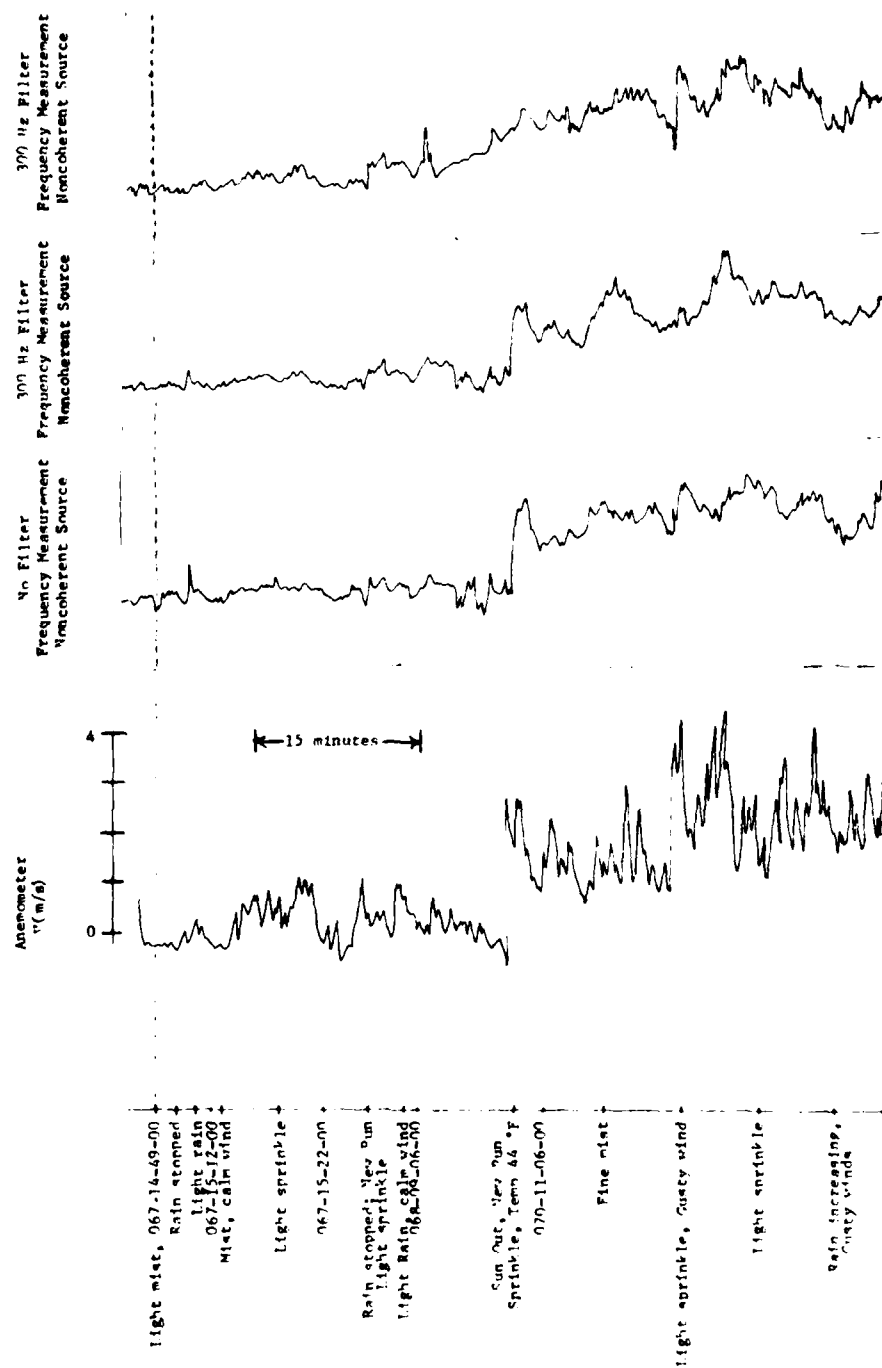


Figure 12. Temporal Filtering Effects on Optically Determined Winds.

March 10, 1980
 Beaverton, Oregon
 Tape #3 - Coherent Beam Source

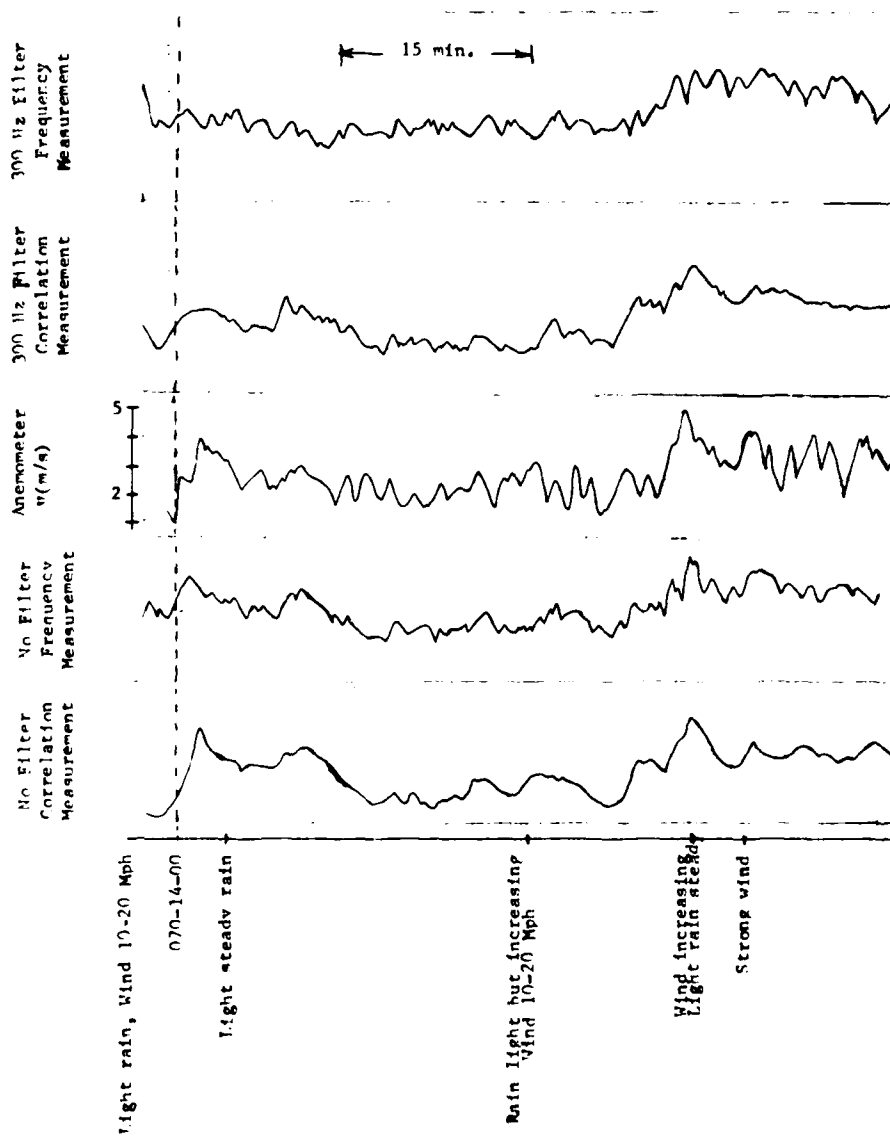
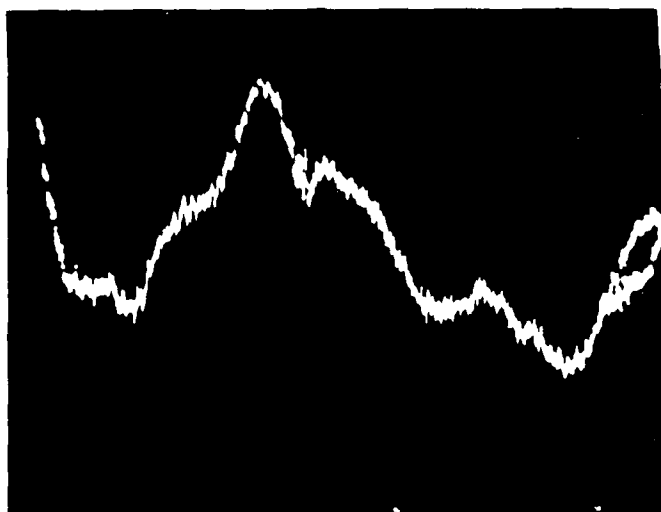


Figure 13. Temporal Filtering Effects on Optically Determined Winds.

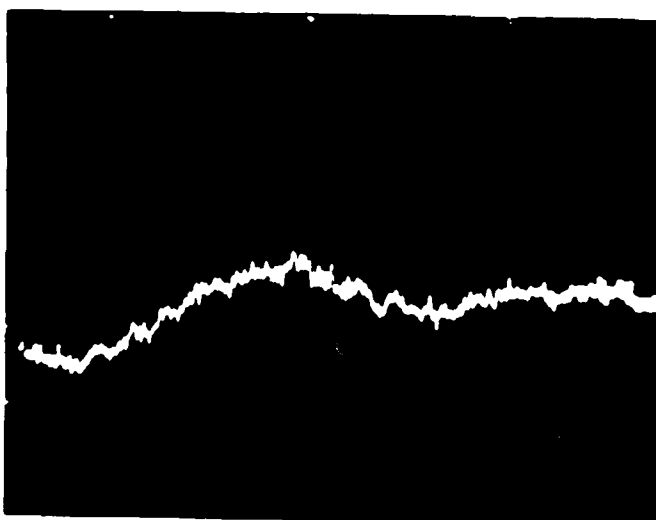
results. The high frequency details of the 300 Hz filtered, zero crossing measurement were not well matched to the anemometer although the low frequency content appeared to match.

Figures 14(a) through 14(c) show photographs obtained from oscilloscope displays illustrating examples of signals obtained from coherent beams, Fig. 14(a) is a "no rain" case taken at 20 m /cm sweep time, and .02 v/cm sensitivity. Similarly, Fig. 14(b) is a "no rain" signal taken at 5 m /cm sweep and .02 v/cm and Fig. 14(c) is a "rain" signal taken at 5 m /cm sweep, and .005 v/cm. The condition represented by the photos was light rain, about .01 in/h . The rain induced signals have a fundamental frequency of above about 1000-1400 Hz.

The spectra obtained from the detected coherent optical signals in the presence of rain and under "no rain" conditions are shown in Figs. 15(a) through 15(e). The "no rain" results were obtained when wind speeds were about 1 m/s and are shown in (a) through (c). During the rain intervals, Figs. 15(d) through 15(e) the winds were 2-3 m/s. In general the high frequency tail shows a slight slope in the rain cases. This slope is not present in the "no rain" cases.

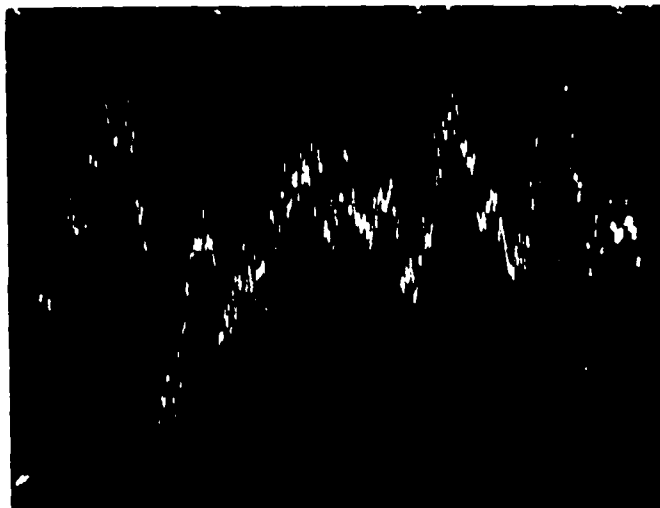


20 ms/cm = .02 V/cm
(a)



20 ms/cm = .02 V/cm
(b)

Fig. 14.
Detected Optical Signals
Natural Light



5 ms/cm - .005 V/cm
(c)

Fig. 14.
Detected Optical Signals
Natural Rain

Data Date and Time: 067-15-01-40
Exp. 7.5 in/s
Coherent Source

Bandwidth: 300 Hz
Freq. Span/div: 0.2 KHz
Sweep Time: 5 sec
Input Sens: 2.0 V
Amp mode: 10 db

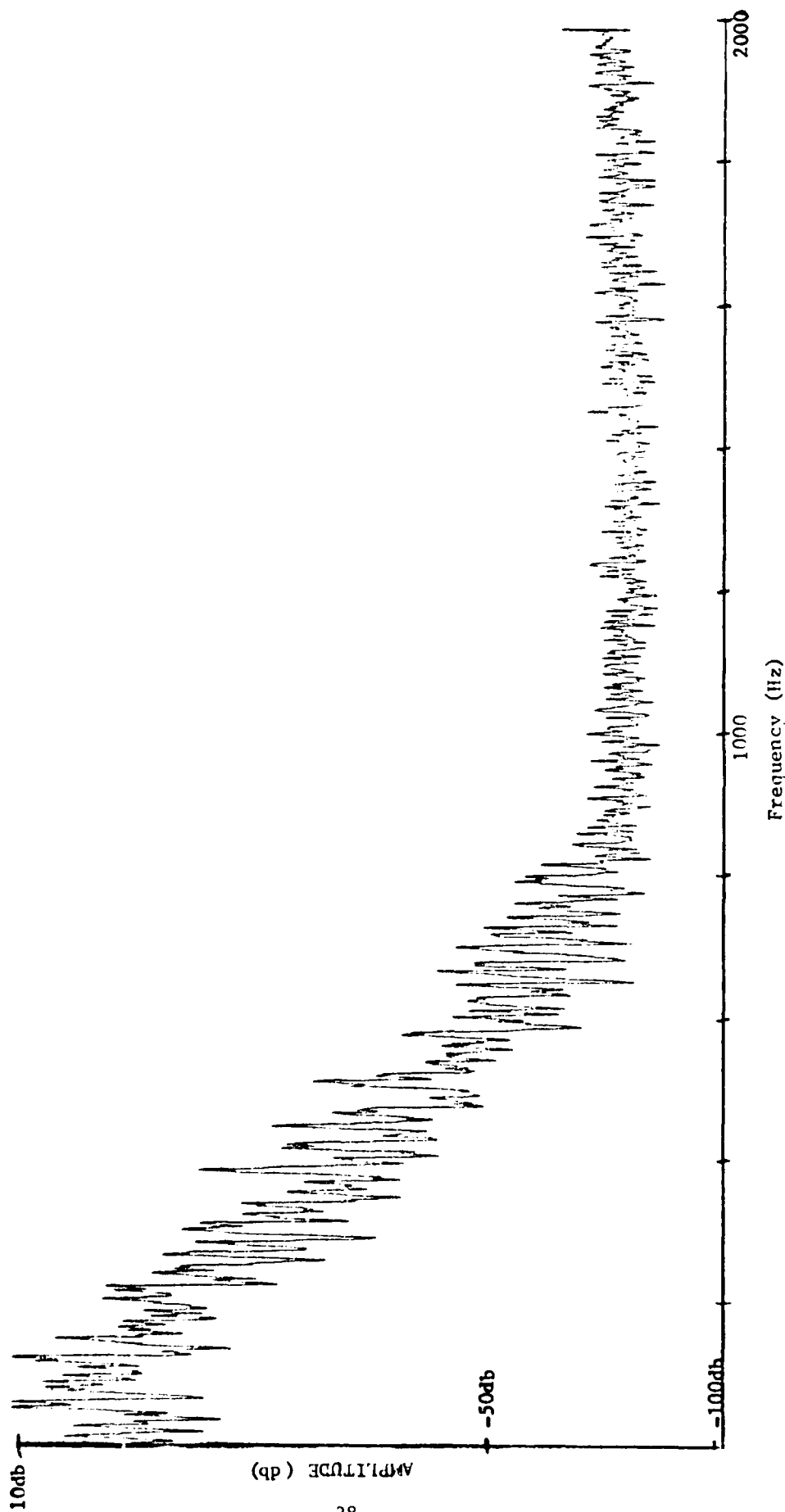
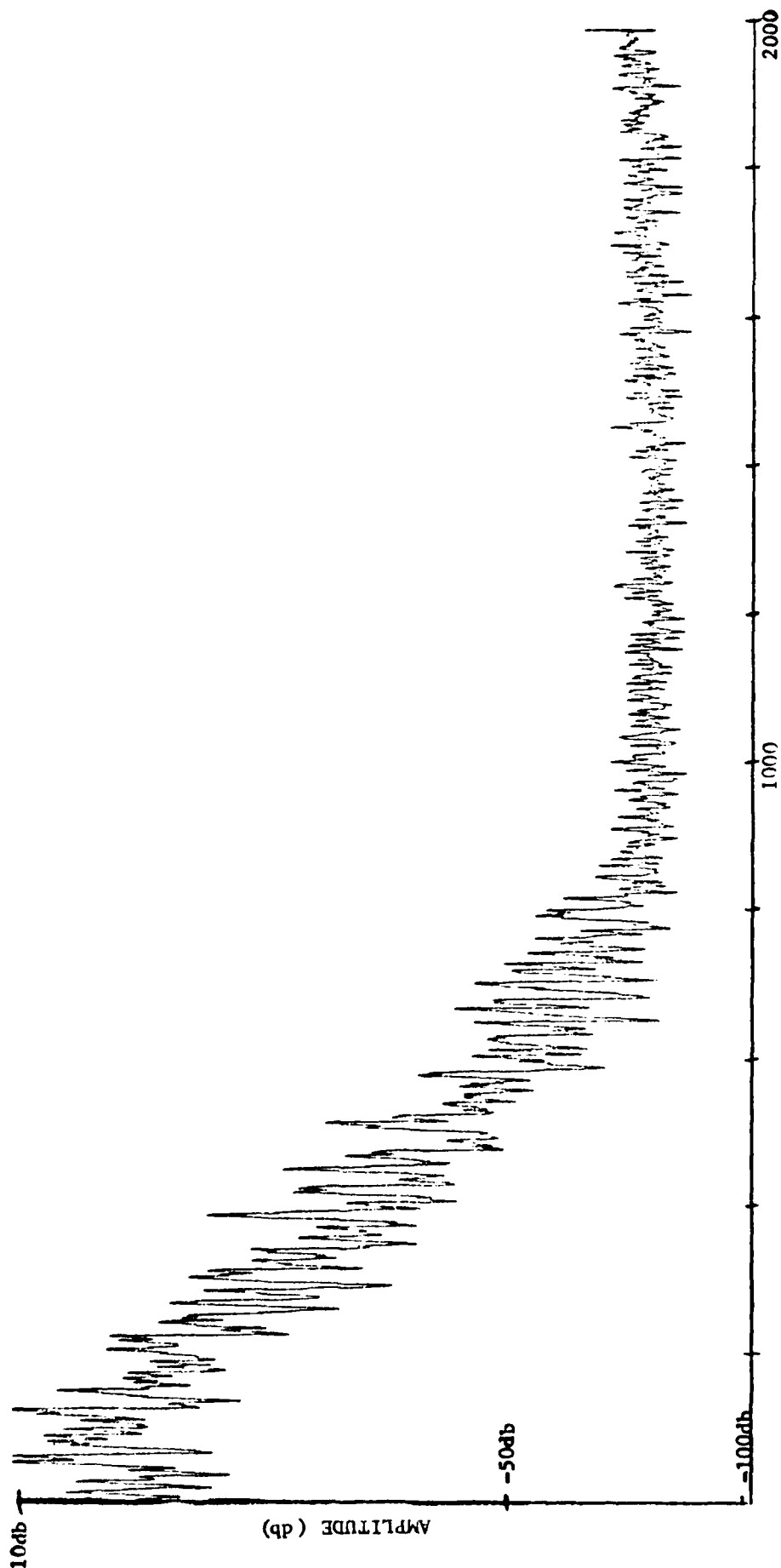


Fig. 15a.

Optical Signal Spectra (Beaverton)

Data Date and Time: 067-15-01-40
Exp. 7.5 in/s
Coherent Source

Bandwidth: 300 Hz
Freq. Span/div: 0.2 KHz
Sweep Time: 5 sec
Input Sens: 2.0 V
Amp mode: 10 db



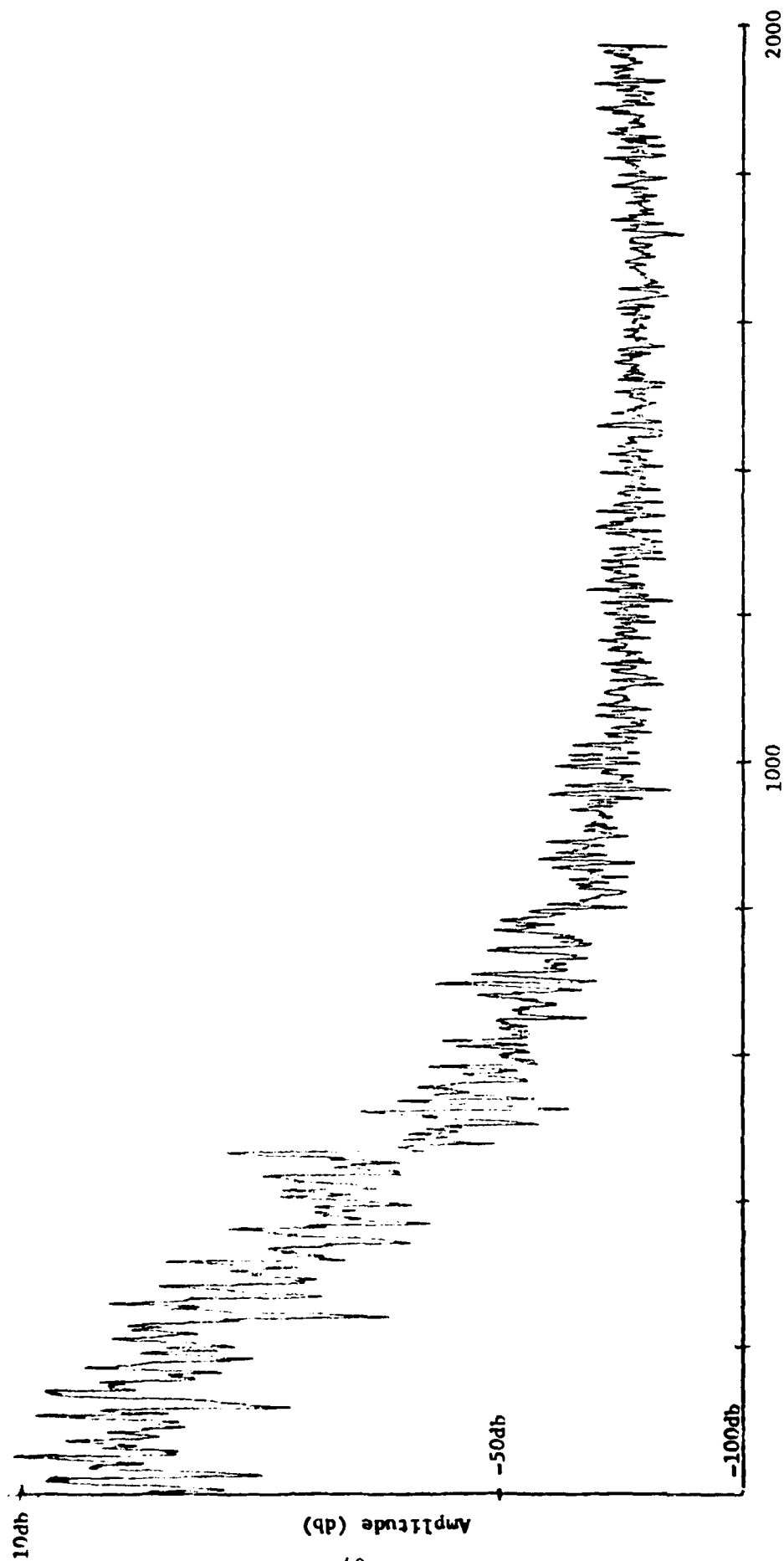
Frequency (Hz)

Fig. 15a.

Optical Signal Spectra (Beaverton)

Data Date and Time: 067-14-50-00/50
Exp. 7.5 in/s
Coherent Source

Bandwidth: 300 Hz
Freq. Span/div: 0.2 KHz
Sweep Time: 5 sec/div
Input Sens: 2.0 V E
Amp mode: 10 db



Frequency (Hz)

Fig. 15b.

Data Date and Time: 067-14-49-00
Exp. 7.5 in/s
Coherent Source

Bandwidth: 300 Hz
Freq. Span/div: 0.2 KHz
Sweep Time: 5 sec/div
Input Sens: 2.0 V
Amp mode: 10 dB

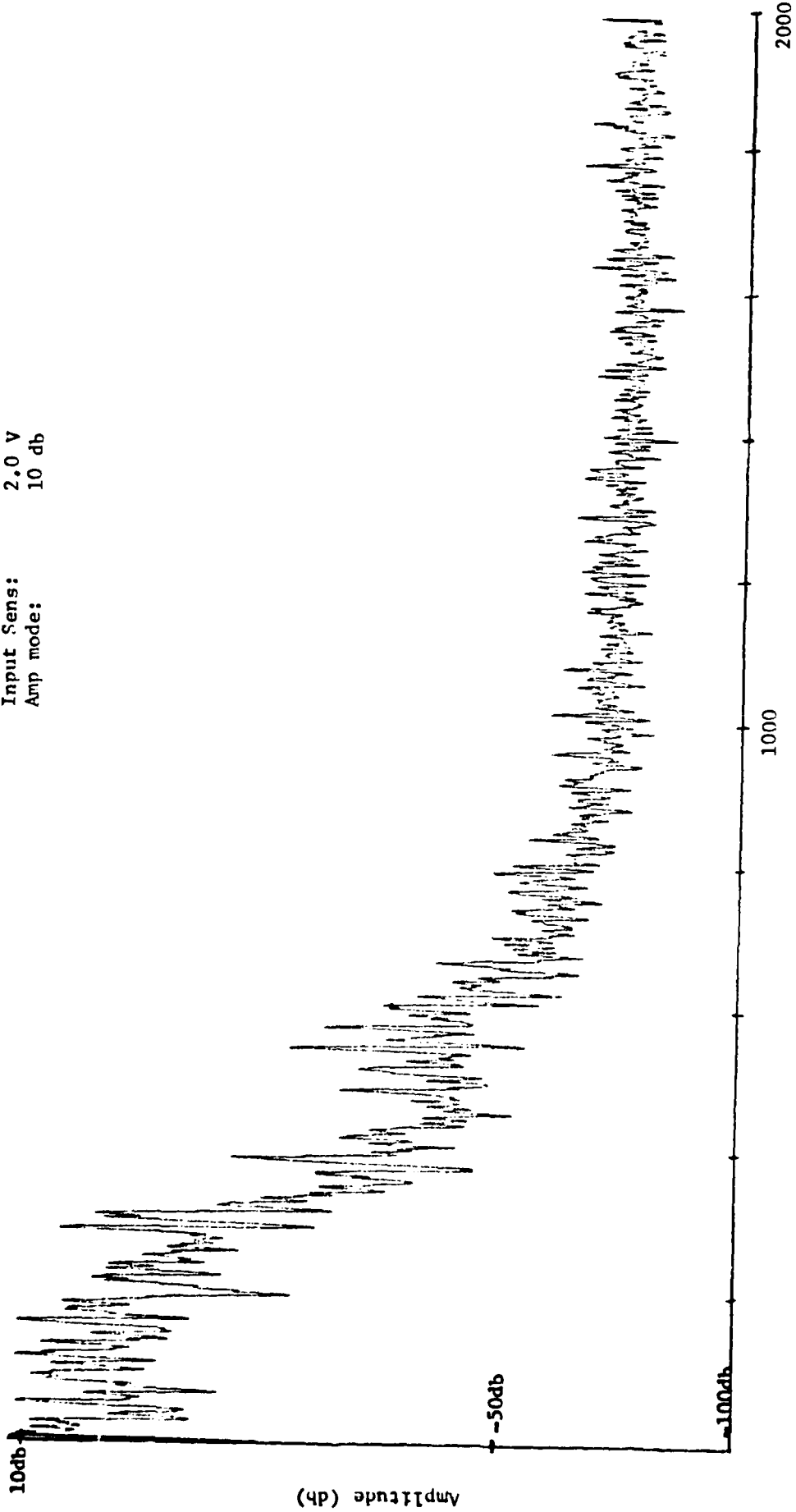


Fig. 15c.

Data Date and Time: 070-13-58-00/50
Exp. 7.5 in/s
Coherent Source

Bandwidth: 300Hz
Freq. Span/div: 0.2 KHz/div
Sweep Time: 5 sec/div
Input Sens: 1.0 V
(Rain)
Amp mode: 10 db

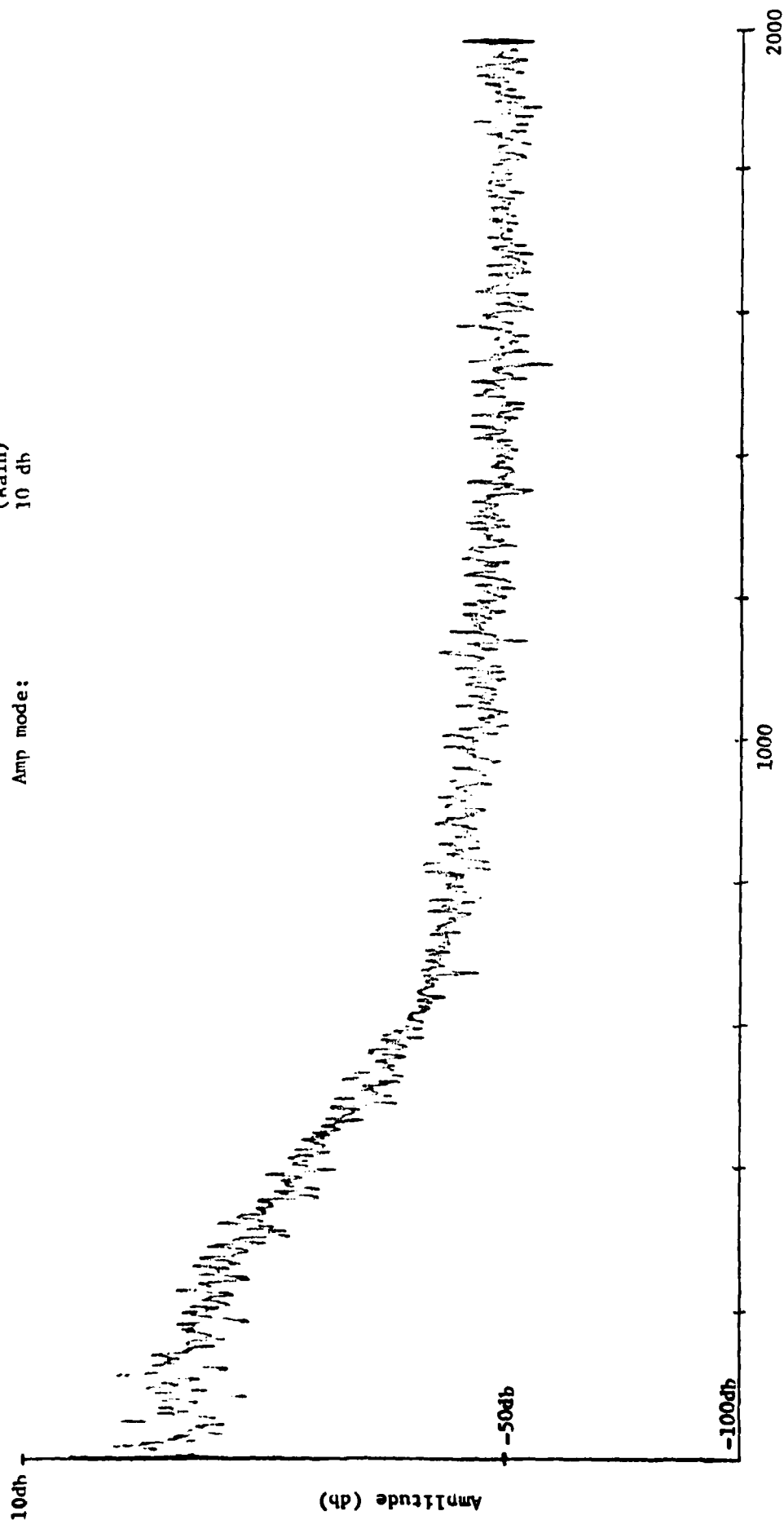


Fig. 15d.

Data Date and Time: 070-14-30-00/50
Exp. 7.5 in/s
Coherent Source

Bandwidth: 300 Hz
Freq. Span/div: 0.2 KHz
Sweep Time: 5 sec/div
Input Sens: 1.0 V
(Rain)
Amp mode: 10 db

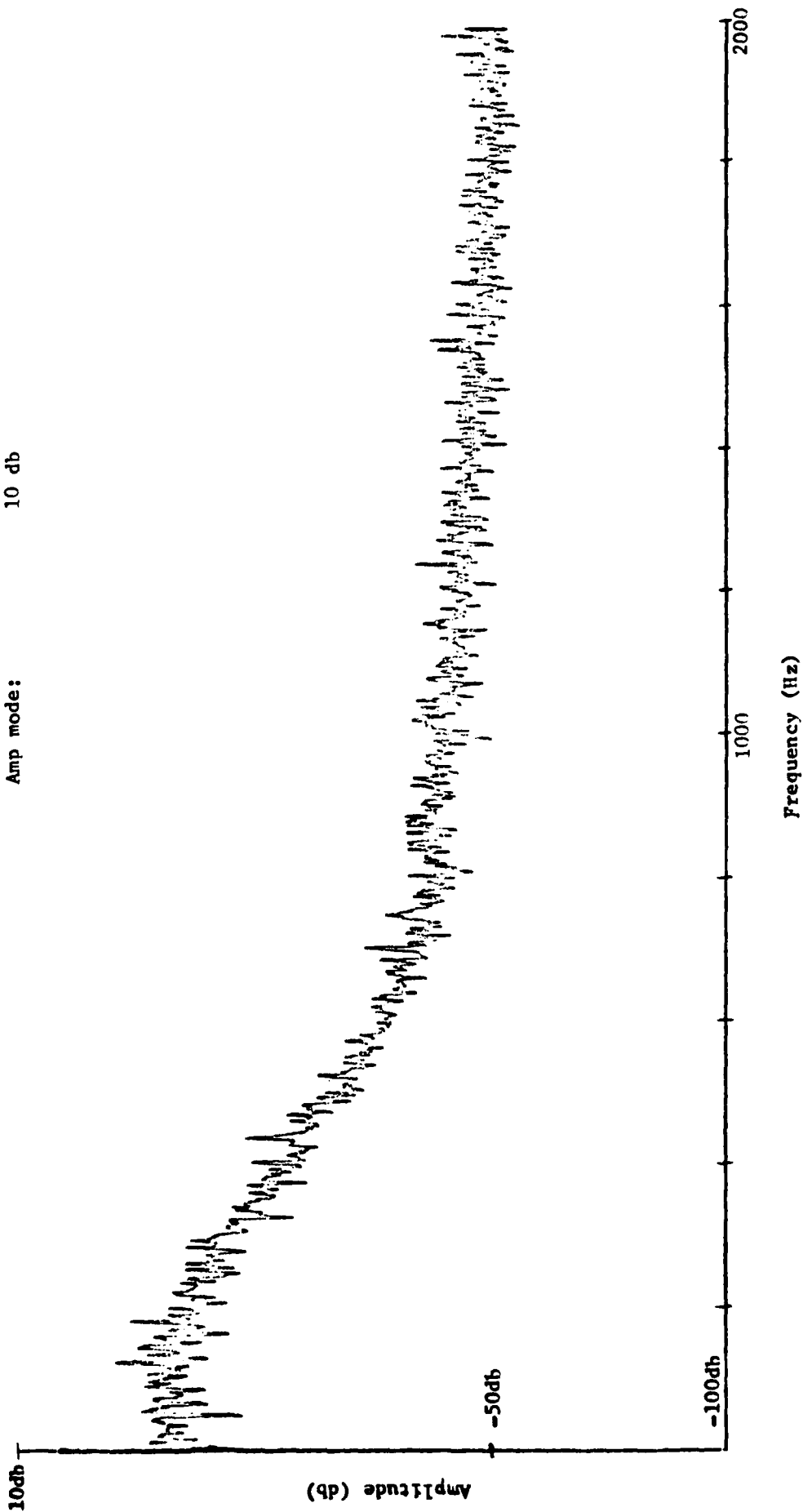


Fig. 15e.

Data Date and Time: 070-14-00-00/50
Exp. 7.5 in/s
Coherent Source

Bandwidth: 300 Hz
Freq. Span/div: 0.2 KHz
Sweep Time: 5 sec/div
Input Sens: 1.0 V
(Rain)
Amp mode: 10 db

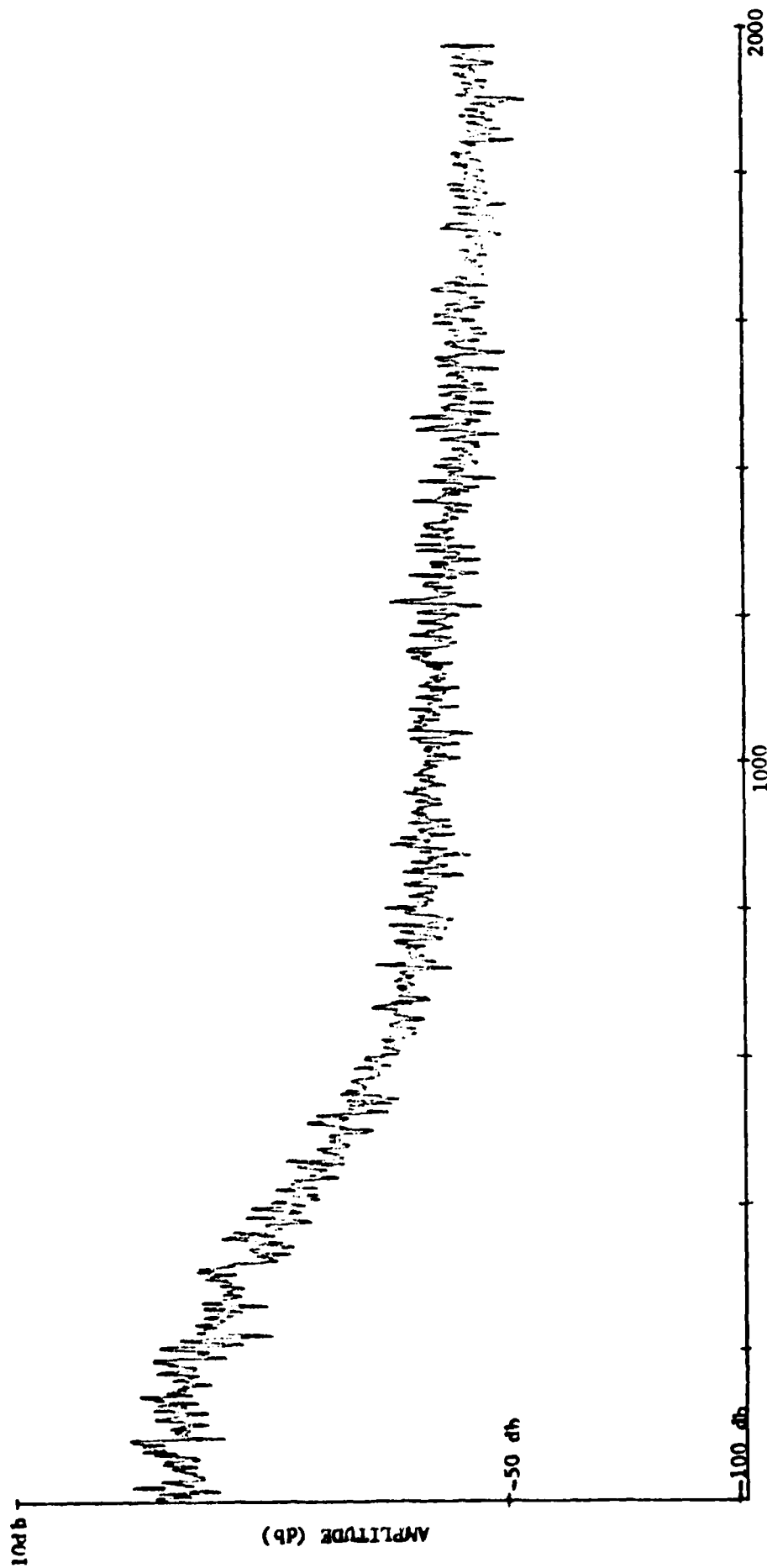


Fig. 15f.

Data Date and Time: 070-14-02-00/50
Exp. 7.5 in/s
Coherent Source

Bandwidth: 300 Hz
Freq. Span/div: 0.2 KHz
Sweep Time: 5 sec/div
Input Sens: 1.0 V
(Rain)
Amp mode: 10 db

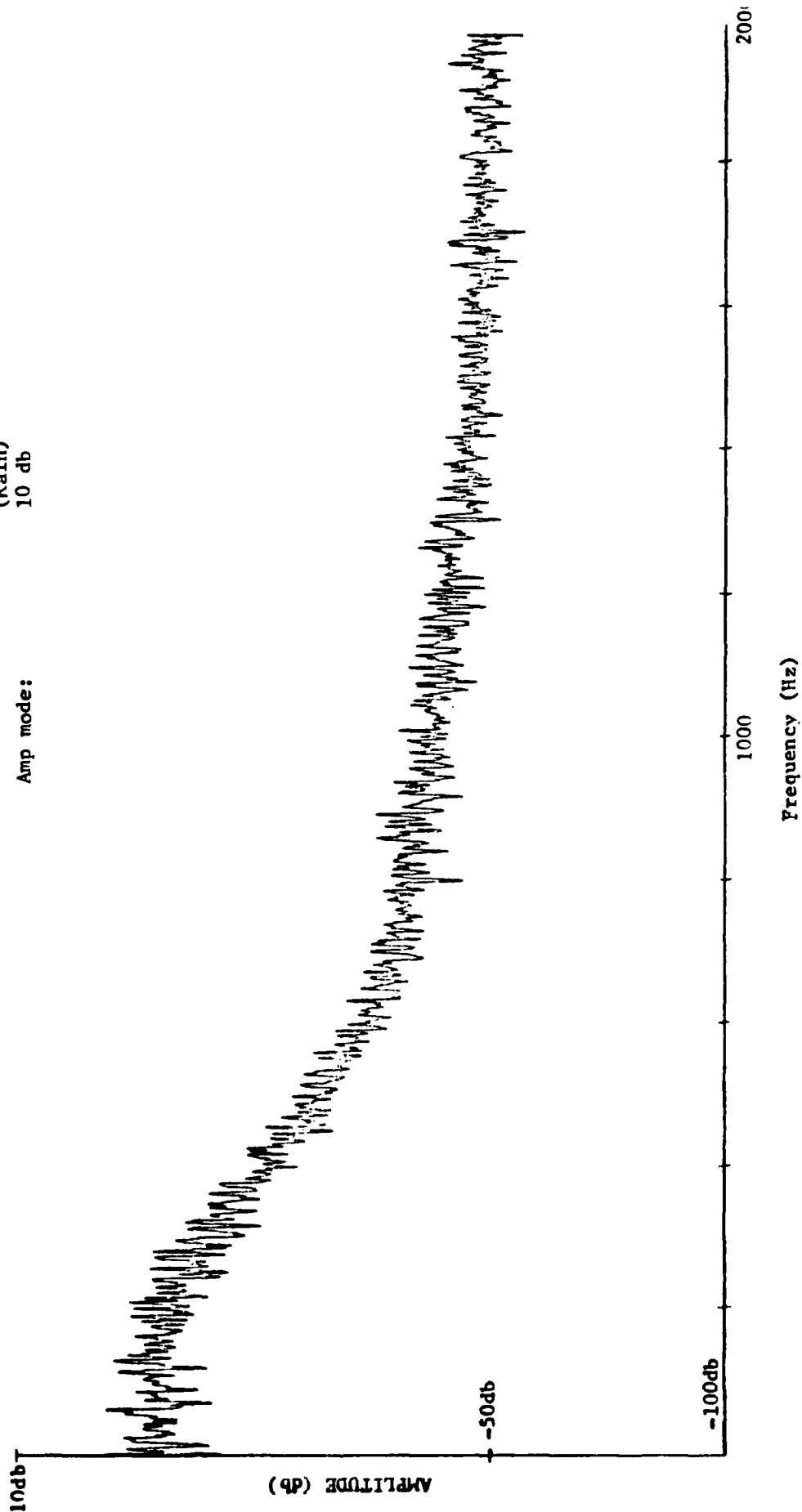


Fig. 158.

1.4 Discussion of Results

The field test data were limited in that only a few different weather conditions were experienced during the tests. At Holloman AFB only light winds were experienced all during the tests. At Beaverton only light rains and generally low winds were obtained. No severe conditions were encountered

However, the data obtained do indicate that temporal low pass filtering of the optical signals can improve the performance of the optical anemometers. The lower limit on the filter cutoff frequency is determined by the desired maximum speed measurement. The signal frequency components displaying the maximum power are given by (*)

$$f = \frac{2u}{\sqrt{2\pi\lambda L}}$$

where u is the crosswind speed in m/s, λ the wavelength, and L is the optical path length. For a HeNe laser beam propagating over a 1 km path this yields $f \approx 22u$. For a maximum desired speed measurement of 20 m/s the filter cutoff should be no lower than 450 Hz. Thus at high wind speeds temporal filtering could degrade the performance of optical anemometers.

The optical signal processors are simple digital devices. As a consequence the low amplitude rain signal will cause no problem except when the signal is near its average value. At this point rain signal can cause the processor to switch polarity. This will cause an "error" in the correlation measurement of speed or an "error" in the zero crossing measurement. As a consequence a minimum signal

level induced by the turbulence relative to the rain noise is required. The data collected during these experiments do not allow determination of this signal to noise ratio.

Optical processors generally obtain a speed estimate from a measurement of a characteristic of the correlation function. It was generally found that measurement of the zero crossing frequency gave a good estimate of the wind speed. The electronic hardware required for the latter processor is much simpler than the former.

The lower frequency limit on the filter may prove impractical if high wind speed measurements are desired. It would also be possible to overcome some of the rain effects by using spatial filters composed of photodiodes arrays. While the spatial filter would alter the weighting of the wind speed along the path in the resultant measurement, it would help eliminate the effects of rain.

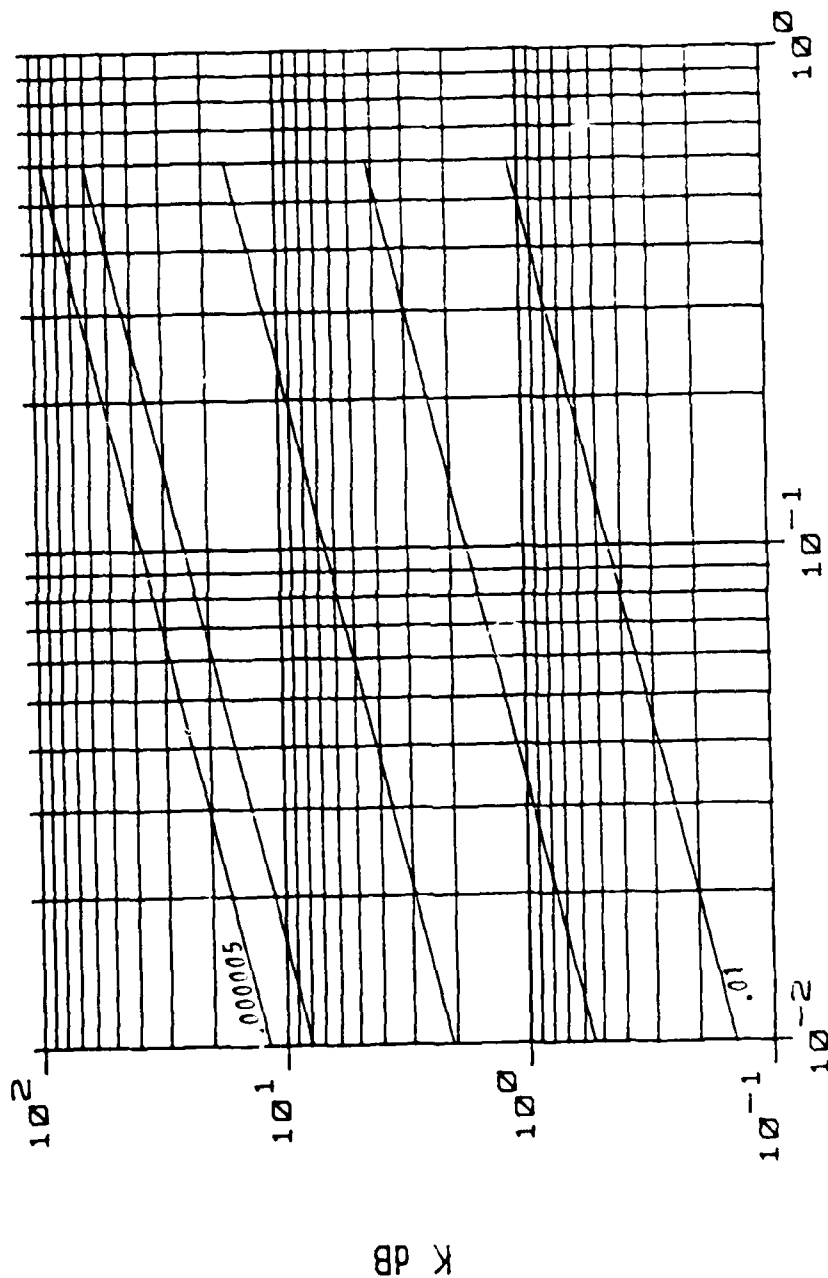
1.5 Scintillations at Millimeter Wavelengths

Estimates of the intensity fluctuations due to temperature inhomogeneities only, at millimeter and submillimeter wavelengths are compared with those expected at optical wavelengths. These estimates were developed on the assumption that wavelength scaling of optical results would hold into the millimeter and shorter range. The calculations also assumed a path length of 30 km for the millimeter waves and a 1 km path length for the optical beam. Figure 16 gives the intensity fluctuation estimate at the longer wavelengths for a specified log amplitude variance, $C_\ell(0)$, of the optical signal.

The expected fluctuation for a 35 GHz wave propagating over a 30 km path would be about 1 db if an optical beam had a $C_\ell(0) = .1$ over a 1 km path. This compares to the intensity fluctuation, typically 1 db but at times as much as 10 db, observed in 35 GHz propagation over a 28 km path which was partially over water^(5,6). While a fairly large receiving antenna was used in the above observation, a linear dimension of about 40 wavelengths, little aperture averaging was predicted⁽⁷⁾. However, it is expected that the humidity variations would have dominated at 35 GHz and that the measured fluctuations would be on the order of 10 db rather than 1 db as observed and as predicted for temperature effects alone.

Using a relationship given by Weslev⁽⁸⁾ the refractive index variations at microwave frequencies can be related to the humidity structure coefficient. If the structure coefficients for temperature and humidity were numerically equal the humidity structure parameter would be a factor of 5 more effective than the temperature parameter

λ (mm) $m = .01, .001, .0001, .00001, .000005$ (METERS)



$C, (\text{Ø}) \text{ opt}$

Fig. 16.

Expected Scintillation (Temperature Effects)

in producing refractive variations at microwave frequencies.

Calculations for a 94 GHz wave propagating over a 2 km path subject to humidity fluctuations yielded 2 db intensity fluctuations. Using this point as a reference the expected intensity fluctuations at other wavelengths can be estimated. These values are shown in Fig. 17.

The above reference value if extended to the 35 GHz wave propagating over a 28 km path would produce fluctuations about 4 db greater than the highest observed fluctuations⁽⁵⁾. While there is some discrepancy between these values, no information was reported on the value of the humidity parameter during the 35 GHz propagation experiment. At the path heights involved the humidity structure parameter may have been somewhat smaller than the value used in the 94 GHz calculation.

While the above discussion indicates that the scintillation effects in millimeter waves can be measured over path lengths on the order of 1 km, it may be desirable to separate temperature and humidity effects by dual frequency propagation experiments.

Wavelength scaling of turbulence induced scintillation yielded values for millimeter waves which are within a range observed and within a range expected from direct calculation. The calculations, Fig. 16 and 17, would only apply to wave frequencies within the propagation windows.

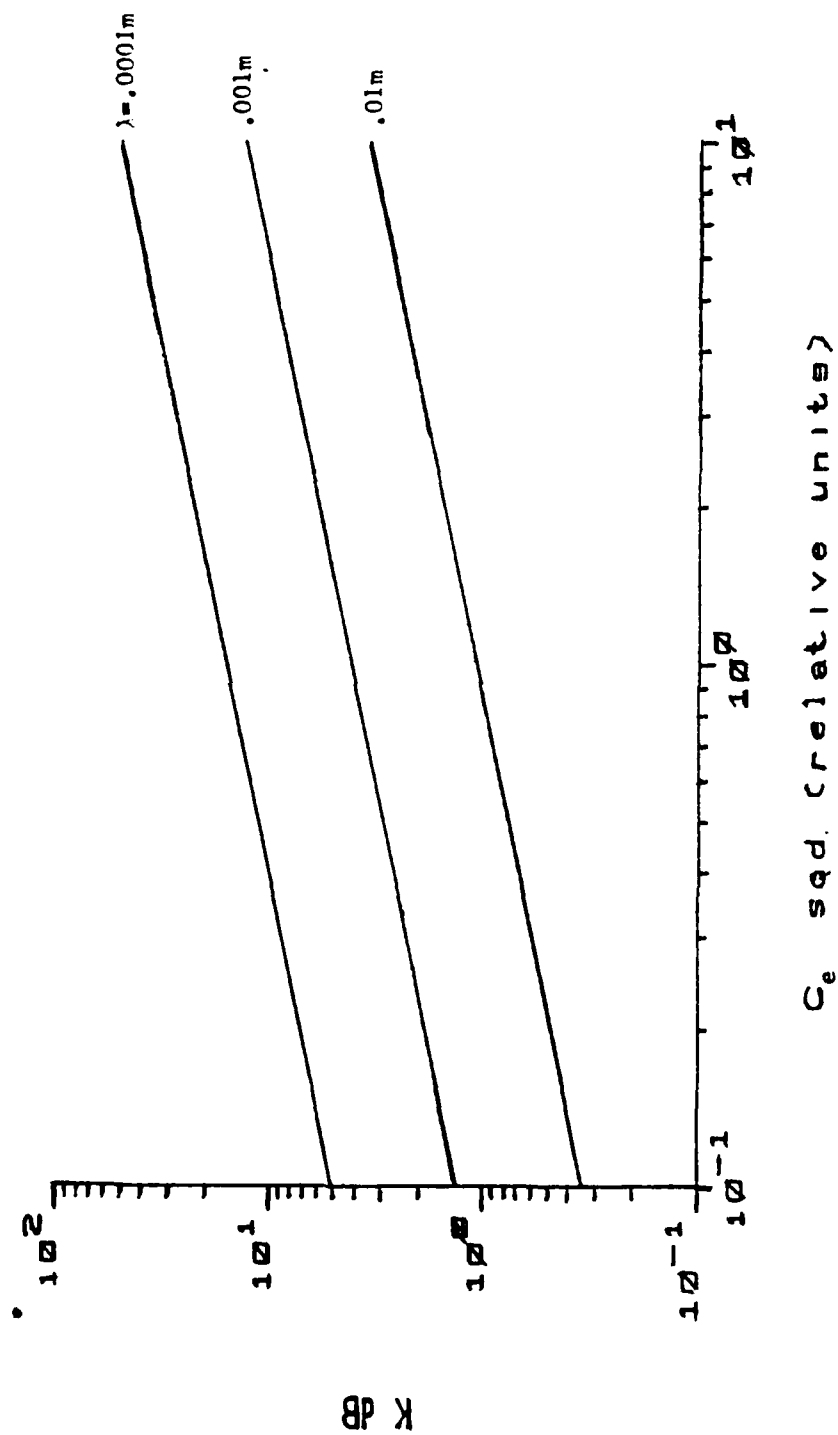


Fig. 17. Expected Scintillation (Humidity Effects)

2.0 IMPORTANT RESULTS

The following observations are considered significant:

Low pass filtering of turbulence induced signals to reduce the rain signal can improve the performance of optical wind sensing systems under light rain conditions.

A frequency measurement of the turbulence induced optical signal yielded representations of the wind speed which matched the speeds obtained from an anemometer. This type of processor yields a real time measurement and the hardware requirements are simple and minimal.

Low pass filtering imposes an upper limit on the maximum wind speed which can be measured with the optical systems. The use of spatial filtering in the receiver could reduce the rain induced effect and not be subject to the maximum speed limitation. This later technique was not evaluated.

Estimates of intensity fluctuations for millimeter waves in the propagation windows indicate that the techniques and processing used at optical frequencies is applicable to the longer wavelengths.

Wavelengths scaling of temperature and water vapor induced signal fluctuations at optical and millimeter wavelengths in the propagation windows, yielded results comparable to those observed in a 35 GHz test.

3.0 REFERENCES

1. Lawrence, R.S., Ochs, G.R., and Clifford, S.F., "Use of Scintillations to Measure Average Wind Across a Light Beam," Appl. Opt. 11, p. 239, (1972).
2. Smith, J., "Wind Measurement Using Optical Beam Position Fluctuations," Trans. Am. Geophys. Union 59, p. 1089, (1978).
3. Ochs, G.R., Bergman, R.R., and Snyder, J.R., "Laser-Beam Scintillation over Horizontal Paths from 5.5 to 145 Kilometers," JOSA, Vol. 59, p. 231, (1969).
4. Clifford, S.F., "Temporal-Frequency Spectra for a Spherical Wave Propagating through Atmospheric Turbulence," JOSA, Vol. 61, p. 1285, (1971).
5. Lee, R.W., and Waterman, A.T. Jr., Space Correlations of 35 GHz Transmissions over a 28 km Path, Radio Science, Vol, 3, #2, p. 135.
6. Lee, R.W., and Waterman, A.T. Jr., A Large Antenna Array for Millimeter Wave Propagation Studies, Proc. of IEEE, April 1966, p. 454.
7. Fried, D.L., Aperture Averaging of Scintillation, JOSA, Vol, 57, #2, p. 169.
8. Wesely, M.L., The Combined Effect of Temperature and Humidity Fluctuations on Refractive Index, Jour. of App. Meteor., Vol. 15, p.43.

DATE
FILMED
-8